A novel method to simulate the 3-D chlorophyll distribution in marine oligotrophic waters

H. Awada[a], S. Aronica[a,*], A. Bonanno[a], G. Basilone[a], S. W. Zgozi[b], G. Giacalone[a], I. Fontana[a], S. Genovese[a], R. Ferreri[a], S. Mazzola[a], B. Spagnolo[c,d,e], D. Valenti[c], G. Denaro[f]

a Istituto per lo studio degli Impatti Antropici e Sostenibilità in ambiente marino (IAS), CNR, S.S. di Capo Granitola, Via del Mare 3, I-91020 Campobello di Mazara (TP), Italy
b Marine Biology Research Centre (MBRC), P.O. Box 30830, Tajura, Libya
c Dipartimento di Fisica e Chimica "Emilio Segrè", Università di Palermo, Group of Interdisciplinary Theoretical Physics and CNISM, Unità di Palermo, Viale delle Scienze, Ed. 18, I-90128 Palermo, Italy
d Istituto Nazionale di Fisica Nucleare, Sezione di Catania, Via S. Sofia 64, I-90123 Catania, Italy
e Radiophysics Department, Lobachevsky State University of Nizhni Novgorod, Gagarin Avenue 23, 603950 Nizhni Novgorod, Russia
f Istituto per la Ricerca e l'Innovazione Biomedica (IRIB), CNR, Via Ugo La Malfa 153, I-90146 Palermo, Italy

* Corresponding Author: salvatore.aronica@cnr.it

Abstract

A 3D advection-diffusion-reaction model is proposed to investigate the abundance of phytoplankton in a difficult-to-access ecosystem such as the Gulf of Sirte (southern Mediterranean Sea) characterized by oligotrophic waters. The model exploits experimentally measured environmental variables to reproduce the dynamics of four populations that dominate phytoplankton community in the studied area: Synechococcus, Prochlorococcus HL, Prochlorococcus LL and picoeukaryotes. The theoretical results obtained for phytoplankton abundances are converted into *chl-a* and *Dvchl-a* concentrations, and the simulated vertical chlorophyll profiles are compared to the corresponding experimentally acquired data during the MedSudMed-08 oceanographic survey. Non parametric tests showed that the 3D model successfully simulates the spatial distribution of chlorophyll in most of the Gulf of Sirte. Statistical analysis indicates that about 80% of the simulated chlorophyll vertical profiles are not significantly different from the experimental data. This model is also a useful tool to predict chlorophyll distributions in hard-to-access areas, where experimental data cannot be collected. Moreover, the model could be used to predict the effects of global warming on phytoplankton dynamics and primary production in marine ecosystems.

Keywords: Spatial ecology, Marine ecosystems, Phytoplankton dynamics, Chlorophyll distribution

1. Introduction

Phytoplankton are the foundation of the marine food web, and represents an important part of the primary producers [1, 2, 3]. It feeds, directly or indirectly, all the aquatic ecosystems from microscopic zooplankton organisms to large marine species. The identification of the spatio-temporal behaviour of phytoplankton groups can give powerful tool to investigate the ocean role in climate regulation in the context of the global change [4] as well as the dynamics of the marine food web and specially the lower levels as the small pelagic species which fed at the basis of the food chain. Fish species distribution and abundance observed in marine ecosystems can be explained by fluctuations in the chlorophyll concentration, which is a marker of the presence of phytoplankton communities [5,

6]. Specially fishes at lower trophic levels like sardine and anchovy have been recognized to be heavily linked to chlorophyll variability specially in their reproductive and growth biology [7, 8], as well as in their high interannual biomass fluctuation and spatial distribution also in the study area [9, 10]. Therefore, modeling phytoplankton dynamics becomes crucial for future ecosystem-based modeling of stock assessment. Phytoplankton are photosynthetic organisms, which require dissolved inorganic nutrients and light, and use chlorophyll to capture sunlight and transform it into chemical energy by photosynthesis [11]. Besides, it is the main driver of the biological carbon pump because the formation of organic matter during the phytoplankton photosynthesis process causes the removal of carbon dioxide (CO_2) dissolved in seawater and the release of oxygen (O_2) in the atmosphere [12]. Through photosynthesis, phytoplankton provides a sink for atmospheric CO_2, favouring its atmosphere-biosphere cycle and controlling Earth's climate [13, 14]. Phytoplankton contributes to almost half of the global primary production [15], on a scale equivalent to all land plants and forests, although it accounts to approximately 1% of the photosynthetic biomass on Earth [16].

Given the overwhelming importance of phytoplankton on the world's ecosystem, it is imperative to consider its variations and how these can be linked to an increase in temperature due to climate change. Indeed, the distribution, abundance phenology and productivity of phytoplankton communities are changing in response to ocean warming, acidification, and stratification [17, 18]. For this reason, the long-time-series observation of the response of phytoplankton to climate change is very important to improve the existing predictive framework in managing and conserving marine ecosystems [17, 19].

In general, the in-situ marine observations of phytoplankton are characterized by relatively high precision. However, such methods sometimes have large gaps and the construction of large-scale data set from these observations is not reliable, especially in hard access unexplored areas.

Consequently, in-situ observations cannot be representative for relatively big areas due to large voids, marine physical heterogeneity and the complex dynamic nature of marine environments.

Other in situ observation methods such as the autonomous profilers are suited for continuous and long-time series (seasons or even years) monitoring of the vertical distributions of marine parameters at specified sites [20]. However, the cost of operating and maintaining such autonomous systems is still expensive [21].

Reconstruction through a modeling approach starting from remote sensing data integrated with the periodic collection of environmental variables can give added value to assess phytoplankton productivity dynamics and chlorophyll stocks. In the last decades, the use of remote sensing (RS) and ocean colour observation techniques led to a better understanding of the phytoplankton dynamics in the upper ocean [4, 22, 23, 24]. However, the use of ocean colour observations provides chlorophyll concentration data only for the near-surface layers of the marine environment [25, 26, 27]. In particular, it was estimated that such techniques can only represent one-fifth of the euphotic layer where phytoplankton photosynthesis takes place [28]. Consequently, in last years the phytoplankton dynamics has been investigated by different modeling approaches [29, 30, 31, 32, 33, 34].

In order to analyse the phytoplankton dynamics, we recall that marine ecosystems are complex open systems, which are characterized by nonlinear interactions among their parts and external perturbations, not only deterministic but also random, coming from the environment [5, 29, 35]. Complex systems are present in different scientific areas among which microbiology, biophysics and biogeochemistry [30, 35, 36]. In our work, we investigate a complex ecosystem, such as the Gulf of Sirte, using a 3D model in which only deterministic perturbations are considered.

In last decades, the spatio-temporal distributions of phytoplankton were often reproduced by one-dimensional biological-physical models [25, 29, 32, 37, 38, 39, 40, 41]. Here, the dynamics and response of phytoplankton species to the light and nutrient availability was intensively investigated in accordance with previous works [42, 43, 44]. For example, Wroblewski et al. [44] studied the response of an initial phytoplankton patch to the stresses of turbulent diffusion, nutrient depletion, light periodicity, and nocturnal or continuous herbivore grazing. Afterwards, several authors investigated the one-dimensional phytoplankton distribution and competition for light and nutrients

using advection-reaction-diffusion models [5, 29, 38, 45, 46]. Similar models were used to reproduce the two and three-dimensional dynamics of phytoplankton in homogenous environments where the nutrient concentration and the light intensity were set constant in the whole domain [33]. Complex biogeochemical models were developed in aims of simulating the three-dimensional dynamics of the lower trophic part of the food web and the biogeochemical cycles of the main nutrients in marine ecosystems [30, 47]. Finally, in a recent work, Valenti et al. [34] used a 2D advection-diffusion-reaction model, which includes real values for physical and biological variables, to reproduce the spatial chlorophyll distribution in highly heterogeneous environment, such as Strait of Sicily.

Concerning the analytical approaches for deterministic models, they are limited to coupled advection-diffusion equations without reaction terms [48, 49, 50]. However, very recently, a general 1D analytic solution of the convection-diffusion-reaction-source equation has been obtained using a one-sided Laplace transform, assuming constant diffusivity, velocity, and reactivity [51]. In particular, analytic solutions have been straightforwardly obtained for a combination of the source function and the initial concentration which provides a non-zero singularity pole of the inverse Laplace transform [51]. The extension of analytical approaches to 2D and 3D models is very hard to face, unless particular spatial symmetries exist, allowing to treat analytically these models.

The present study introduces a more practical and realistic three-dimensional advection-reaction-diffusion model to simulate the spatio-temporal distributions of chlorophyll concentration. The model is tested in the Gulf of Sirte (southern Mediterranean Sea), which is characterized by oligotrophic conditions and high incident light intensity during the summer period. Even though the Gulf of Sirte is an important site for the entire Mediterranean basin from a hydrological point of view, it is poorly investigated and information are scarcely available due to political and security reasons. In this context, the used modeling approach makes an important contribution to simulating environmental variables in scarcely explored and remote regions.

The 3D model takes into consideration several physical and biological processes responsible for the spatio-temporal heterogeneity in the studied area. The considered parameters control the competition and coexistence of four different groups of picophytoplankton, namely Synechococcus, Prochlorococcus LL, Prochlorococcus HL and picoeukaryotes. Moreover, the contribution of each phytoplankton group to the local concentration of divinyl chlorophyll a (*Dvchl-a*) and chlorophyll a (*chl-a*) is taken into account. The model results were compared with the experimental data sampled during the MedSudMed-08 oceanographic survey (15-30 July 2008), by performing statistical checks based on the Kolmogorov–Smirnov (K-S) Test.

2. Materials and Methods

2.1. Environmental Data

In this work, we analyse the marine ecosystem of the Gulf of Sirte, which is localized at the eastern basin of the Mediterranean Sea, in the central part of Libyan waters. Specifically, the Gulf of Sirte is a semi-enclosed basin opening to the Mediterranean Sea (see Fig. 5) and covering an area of approximately 75.000 km^2. Here, the diversity of phytoplankton is a result of numerous factors, including nutrients, light, hydrology and biological factors [34, 52]. Among these, Lévy et al. [24] identified the importance of marine currents in shaping marine life and biodiversity in this kind of marine ecosystem.

The environmental data were collected during the MedSudMed-08 oceanographic survey carried out in Libyan waters from 15 to 30 July 2008 on board of the R/V Urania. The sampling was carried out by using a grid of 12 hydrological profiles along the north-south transect of the Strait of Sicily between Cape Passero and Misurata, and of 60 hydrological stations located in Libyan waters and distributed to cover much of the Gulf of Sirte. The vertical profiles of oceanographic parameters, such as conductivity, temperature, pressure, density and dissolved oxygen, were collected along the water

column by means of a CTD-rosette system, consisting of a CTD SBE 911 plus (Sea-Bird Inc.), and a General Oceanics rosette with 24 12 l Niskin bottles [53, 54]. At the same time, the fluorescence data were acquired using a Chelsea Aqua 3 sensor mounted on the probe.
The fluorescence data were subsequently converted into equivalent chlorophyll a concentration (μg/l), and were used to estimate the depth of the deep chlorophyll maximum (DCM) [29, 38, 39].
The samples for nutrients analysis (nitrite, nitrate, silicate and phosphate concentrations) were collected directly from Niskin bottles on the 16 sampling stations that were identified to represent the different hydro-morphologic characteristics in the Gulf of Sirte (see Fig. 5 empty squares). The vertical profiles of the two horizontal components of the marine currents were acquired using a Lowered Acoustic Doppler Current Profiler system (LADCP WH Sentinel of RDI Instruments) and computed by applying the Lamont-Doherty Earth Observatory (LDEO) processing software [55]. All the environmental variables were processed, generating for each site a text file, in which the experimental values are given with a 1 m step [34]. An exception was the nutrients data which were obtained with a 5, 10 and 25 m steps depending on the depth of the water column. The daily incident light intensity at the water surface for the whole period investigated (1 January 2007 - 31 December 2008) was estimated by using the remote sensing data (see the NASA web site http://eosweb.larc.nasa.gov/sse/RETScreen/) according to previous works [5, 6, 34].

2.2. The 3-D advection-diffusion-reaction model

The dynamics of net primary production (NPP) in oligotrophic waters of the Gulf of Sirte is analysed by using a 3D advection-reaction-diffusion model. Specifically, the model allows to reproduce the spatial-temporal behaviour of picophytoplankton abundance ($b_i(x,y,z,t)$) for the four most representative populations in the investigated site, and to calculate simultaneously the theoretical distribution of total *chl-a* concentration. Moreover, the spatial distributions of the nutrient concentration ($R(x,y,z,t)$) and light intensity ($I(x,y,z,t)$) are obtained. In our study, the (x,y,z,t) denotation indicates the spatio-temporal distribution of variables, in which the position on the horizontal plane is described by x and y, the depth of water column is labelled by z, and the time is denoted by t.
The advection-reaction-diffusion model takes into account several biological and hydrological processes [34]: i) net growth (reaction term); ii) passive movement (advection/sinking term); iii) movement due to turbulence (diffusion term).
The reaction term is described by the net phytoplankton growth rate ($G_i(x\,y,z,t)$), which depends on the balance between the gross production rate per capita and the mortality [34]. In particular, the gross production rate per capita is calculated by taking into account the nonlinear interactions between different phytoplankton communities and the inter-specific competition for the two considered limiting resources, i.e., light intensity and nutrients [5, 34, 45], while the mortality due to respiration, death, and grazing is fixed according to previous experimental works [56, 57, 58]. More specifically, the limiting effect of light intensity and nutrient concentration on the phytoplankton growth is considered by Monod kinetics [59], and the gross phytoplankton growth rate is obtained using the Michaelis-Menten formulas [37, 60]. According to this, the net phytoplankton growth rate of the i^{th} picophytoplankton group is defined as follows

$$G_i(x,y,z,t) = \min\left(r_i \frac{R}{R + K_{R_i}}, r_i \frac{I}{I + K_{I_i}} \right) - m_i \qquad (1)$$

where r_i is the maximum growth rate of i^{th} picophytoplankton group; $R(x,y,z,t)$ is the nutrient concentration; $I(x,y,z,t)$ is the light intensity; K_{R_i} and K_{I_i} are the half-saturation constants for nutrient concentration and light intensity, respectively, of the i^{th} picophytoplankton group. In the Gulf of Sirte (Eastern Mediterranean Sea), the phosphates are considered to be the limiting nutrient for the phytoplankton growth [29, 53, 61].

The advection term reproduces the effects of marine currents (local transport process) on the horizontal distribution of picophytoplankton groups, while the sinking term describes the effects of the gravitational force on the vertical distribution of phytoplankton abundances.
The diffusion term reproduces the effects of the turbulence on the three-dimensional distribution of picophytoplankton groups through the horizontal (D_x and D_y) and the vertical (D_z) turbulent diffusivities, which remain constant with the position and the time (see Supplementary Information). The horizontal and vertical turbulent diffusivities are set in accordance with values estimated in previous works [62, 63].
In the model, we also consider that the quantity of nutrient is increased by the recycling process of the dead phytoplankton [34]. Furthermore, the effects of the marine currents and turbulence on the 3D distribution of nutrients are considered by inserting three advection terms and three diffusion terms in the PDE for the phosphate concentration ($R(x,y,z,t)$), respectively.
It is assumed that the intensity of light ($I(x,y,z,t)$) depends on the position (x,y) along the horizontal plane, it decreases exponentially as a function of depth (z) according to the Lambert-Beer's law [64, 65], and changes as a function of time during the year.
With these assumptions, we define the 3D model using the following equations

$$\frac{\partial b_i(x,y,z,t)}{\partial t} = b_i(x,y,z,t)G_i(x,y,z,t) + \frac{\partial}{\partial x}\left[D_x \frac{\partial b_i(x,y,z,t)}{\partial x}\right] + \frac{\partial}{\partial y}\left[D_y \frac{\partial b_i(x,y,z,t)}{\partial y}\right]$$
$$+ \frac{\partial}{\partial z}\left[D_z \frac{\partial b_i(x,y,z,t)}{\partial z}\right] - \frac{\partial}{\partial x}\left[v_x(x,y,z)b_i(x,y,z,t)\right] - \frac{\partial}{\partial y}\left[v_y(x,y,z)b_i(x,y,z,t)\right] \quad (2)$$
$$- \frac{\partial}{\partial z}\left[v_z(x,y,z)b_i(x,y,z,t)\right] - \frac{\partial}{\partial z}\left[v_i b_i(x,y,z,t)\right]$$

$$\frac{\partial R(x,y,z,t)}{\partial t} = -\sum_{i=1}^{4} \frac{b_i(x,y,z,t)}{Y_i} \cdot (G_i(x,y,z,t) + m_i) + \frac{\partial}{\partial x}\left[D_x \frac{\partial R(x,y,z,t)}{\partial x}\right] + \frac{\partial}{\partial y}\left[D_y \frac{\partial R(x,y,z,t)}{\partial y}\right]$$
$$+ \frac{\partial}{\partial z}\left[D_z \frac{\partial R(x,y,z,t)}{\partial z}\right] - \frac{\partial}{\partial x}\left[v_x(x,y,z)R(x,y,z,t)\right] - \frac{\partial}{\partial y}\left[v_y(x,y,z)R(x,y,z,t)\right] \quad (3)$$
$$- \frac{\partial}{\partial z}\left[v_z(x,y,z)R(x,y,z,t)\right] + \sum_{i=1}^{4} \varepsilon_i m_i \frac{b_i(x,y,z,t)}{Y_i}$$

$$I(x,y,z,t) = I_{in}(t)\exp\left\{-\int_0^z \left[\sum_{i=1}^{5} a_i \cdot chla_i(x,y,Z,t) + a_{bg}\right] dZ\right\} \quad (4)$$

with i varying from 1 to 5 and indicating Synechococcus, Prochlorococcus HL, Picoeukaryotes, Prochlorococcus LL and nano- and micro-phytoplankton (>3μm), respectively. Here, D_x, D_y and D_z are the horizontal and vertical turbulent diffusivities; $v_x(x,y,z)$, $v_y(x,y,z)$ and $v_z(x,y,z)$ are the horizontal and vertical components of marine currents measured along the water column; v_i is the sinking velocity of the i^{th} picophytoplankton population; ε_i, m_i , $1/Y_i$ and a_i are the nutrient recycling coefficient, the specific loss rate, the nutrient content, and the *chl a*-normalized average absorption coefficient of the i^{th} picophytoplankton population; a_{bg} is the background turbidity due to non-phytoplankton suspended particulate; $I_{in}(t)$ is the daily incident light intensity at the water surface; $chla_i(x,y,z,t)$ is the *chlorophyll a* concentration corresponding to the abundance of i^{th} picophytoplankton population. All the model parameters are summarized in Table I of Supplementary Information.
The 3D model is completed by a set of equations, which describes the nutrient and phytoplankton fluxes at the boundaries of the Gulf of Sirte. Here, we fix the following conditions for the picophytoplankton abundance and the phosphate concentration: no biomass can enter or leave the area investigated except through the open sea; no nutrient flux is present through the water surface;

the phosphate concentrations at the deepest layer of the water column are fixed equal to the values measured previously in hydrological stations of the Gulf of Sirte; no nutrient flux is present through the lateral surfaces except at the open sea; the picophytoplankton abundance and the phosphate concentration are set constant out of the Gulf of Sirte; the lateral fluxes for picophytoplankton abundance and phosphate concentration at the open sea depend on the behaviour of horizontal velocities. The boundary conditions for the picophytoplankton abundance and the phosphate concentration are defined by the following equations:

$$\left[D_x \frac{\partial b_i}{\partial x} - v_x b_i\right] = \left[D_y \frac{\partial b_i}{\partial y} - v_y b_i\right] = 0, \quad b_i(x_{bou}, y_{bou}, z) = b_{i_{ext}} \tag{5}$$

$$\left[D_z \frac{\partial b_i}{\partial z} - (v_z + v_i) b_i\right]_{z=0} = \left[D_z \frac{\partial b_i}{\partial z} - (v_z + v_i) b_i\right]_{z=z_b} = 0 \tag{6}$$

$$\left[D_x \frac{\partial R}{\partial x} - v_x R\right] = \left[D_y \frac{\partial R}{\partial y} - v_y R\right] = 0, \quad R(x_{bou}, y_{bou}, z) = R_{ext} \tag{7}$$

$$\left.\frac{\partial R}{\partial z}\right|_{z=0} = 0, \quad R(x, y, z_b) = R_{in}(x, y, z_b) \tag{8}$$

where b_{exti} is the average abundance of i^{th} picophytoplankton population in the Strait of Sicily; z_b is the depth of the water column in each position (x,y); R_{ext} is the average phosphate concentration at the boundaries of the Gulf of Sirte; $R_{in}(x,y,z_b)$ is the phosphate concentration at the deepest layer of the water column in each position (x,y).

Equations (1-8) describe the 3D advection-diffusion-reaction model proposed to reproduce the spatio-temporal behaviour of the picophytoplankton abundances, the phosphate concentration and the light intensity in the seawater of the Gulf of Sirte. The model results are used to calculate the theoretical total *chl-a* concentration in the whole 3D domain. The comparison between theoretical findings and corresponding experimental data acquired during the MedSudMed-08 oceanographic survey is very good.

To test the agreement between the observed data and the predicted model results two non-parametric statistical tests were applied. In particular, these tests are used to compare two independent samples overall (Chi Square) and the shape along the vertical profile (Kolmogorov – Smirnov) and obtain the probability of finding simulated results not different from experimental observations (null hypothesis).

3. Results

In our study, the implementation of the numerical methods was done using a C++ program that exploits an explicit finite difference scheme. The numerical integration of partial differential equations (PDEs) was performed using the method of lines (MOL), which allows to discretize separately spatial and temporal domains [66]. The MOL approach is useful to deal with the complicated discretization of three-dimensional model PDEs, in which are included advection terms, diffusion terms and the non-linear reaction terms. Here, the differential equations of the model were solved using a centred-in-space finite difference scheme for the diffusion terms, and a first-order upwind-biased finite difference scheme for the advection and taxis terms. The spatial discretization (Δx = 23.335 km, Δy = 13.519 km and Δz = 5 m) and the temporal step (Δt = 10 min) were chosen to satisfy the stability and convergence conditions for the numerical method used [66, 67]. By this way, the steady state was obtained after a few simulated months (3 months) starting from 1 January 2007. According to previous works [34, 45], the initial distribution of the four picophytoplankton groups was set uniformly over the whole domain with low cell concentrations, while the initial distribution

of phosphate concentration was fixed on the basis of the experimental findings (see Supplementary Information). The advection-reaction-diffusion model was solved over the investigated period between 1 January 2007 and 31 December 2008. The model reproduced the spatio-temporal distribution of phytoplankton abundances (cell·m^{-3}) of the 4 phytoplankton populations by solving numerically the Eqs. (1)-(5).

Next, Prochlorococcus (HL- and LL-ecotype) and picoeukaryotes abundances were converted into chlorophyll concentration by using the conversion curves obtained by Brunet et al. [52] in the Strait of Sicily. Similarly, the *chl-a* concentration associated to Synechococcus was obtained by its *chl-a* cellular content, which was set to 1.18 fg·cell^{-1} by Morel et al. [68] in presence of oligotrophic conditions. Finally, the contribution of nano- and micro-phytoplankton (>3μm) was added to the simulated chlorophyll to obtain the spatio-temporal behaviour of the total *chl-a* concentration for the whole investigated domain.

From a qualitative point of view the theoretical results of the present model on picophytoplankton abundances well reproduced the real spatial distribution of four planktonic groups along the water column [52, 69]. In particular, the Synechococcus was concentrated in shallower layers of the water column, with peaks of abundance (1.09±0.208 ·10^{10} cell·m^{-3}) between 0 and 45 m depth. The Prochlorococcus HL was mainly observed in intermediate layers, with abundance maxima (in average 0.668±0.229·10^{10} cell·m^{-3}) localized between 0 and 75 m depth. The abundance peaks of picoeukaryotes (in average 4.3±1.4 ·10^{7} cell·m^{-3}) were mainly obtained around 95 m depth. The Prochlorococcus LL was mainly observed in deeper layers of the water column, with peaks of abundance (in average 0.668±0.229 ·10^{10} cell.m^{-3}) localized between 100 and 125 m depth. Generally, from a quantitative point of view, these theoretical results are of the same order of magnitude compared to experimental data in the Strait of Sicily [52, 69]. Moreover, these results confirmed further experimental findings, which indicated an increase in Prochlorococcus abundance and decrease in other phytoplankton groups in oligotrophic conditions [69, 70].

The theoretical results on the total chlorophyll concentration indicated the presence of a Deep Chlorophyll Maximum (DCM), ranged between 100 and 150 m of depth, which is in agreement with experimental data acquired in the Gulf of Sirte. In general, the position of the DCM was mainly associated with the composition of the phytoplankton community, different phytoplankton coping capabilities and environmental conditions (light intensity, oligotrophic waters, velocity field, etc).

In order to identify the diverse contribution of picophytoplankton groups to the biomass primary production in terms of *chl-a* and *Dvchl-a* concentration along the water column, the vertical domain was divided into four layers (0-50, 50-100, 100-150 and 150-200 m). As shown in Table 1, picophytoplankton dominated in terms of chlorophyll concentration throughout the euphotic zone and accounted to 77.32%, 91.17%, 95.39% and 79.34% of the total chlorophyll concentration in the four considered layers, respectively. These results agree with the experimental findings of Brunet et al. [69] in the Strait of Sicily, who stated that picophytoplankton fraction accounts approximately to 80% (±10%) of total chlorophyll and those of Yogev et al. [71] that shown the dominance of picophytoplankton in oligotrophic areas.

The structure of the Picophytoplankton community showed a different distribution pattern with depth (see Table 1). Specifically, Synechococcus dominated the other populations in the uppermost layer (0-50 m), contributing to 43.95% of total chlorophyll. Similarly, a chlorophyll concentration relative maximum associated with the Prochlorococcus HL was observed in the shallower layers (0-100 m) of the water column. Picoeukaryotes and Prochlorococcus LL prevailed in the second layer of the water column (50-100 m), where contributed at 31.21% and 38.35% of total chlorophyll concentration, respectively. Prochlorococcus LL dominated over the other picophytoplankton species in the two deeper layers (3rd and 4th) characterized by lower light intensities, where contributed at 77.51% and 63.97% of total chlorophyll concentration, respectively. On the whole, these theoretical results are in agreement with experimental findings of the Mediterranean basin, where it was shown that Synechococcus dominated numerically the upper 50 m, while Picoeukaryotes and

Prochlorococcus (HL and LL) were significantly more abundant at DCM (between 50 and 100 m) [70, 72].

In Fig. 1, we show the two-dimensional distributions of total chlorophyll concentration obtained by model for five selected depth levels (2.5, 47.5, 97.5, 147.5 and 197.5 m). Here, we observe low values of chlorophyll concentration, ranging between 0 and 0.05 $mg \cdot m^{-3}$, at 2.5 and 47.5 m depth in correspondence of the Synechococcus abundance peak. On the contrary, higher total chlorophyll concentrations (up to 0.18 $mg \cdot m^{-3}$) are obtained at 97.5 m depth, with a chlorophyll maximum localized in the south-eastern side of the Gulf of Sirte. Although Prochlorococcus HL exists at this depth, this population does not contribute significantly to the total chlorophyll concentration, which is mainly due to the abundance peak of picoeukaryotes and the high contribution of Prochlorococcus LL. In deeper levels (147.5 and 197.5 m) chlorophyll concentration is uniformly distributed in the whole 2D domain and is mainly formed of Prochlorococcus LL. This species prevails in deeper layers due to better adaptability to environmental conditions (light limitation and oligotrophic waters), compared to other phytoplankton populations [72]. In general, higher chlorophyll concentrations are obtained in the southern part of the Gulf of Sirte, close to Libyan coast. This spatial distribution is probably due to both the transport of nutrients caused by the Atlantic Libyan Current (ALC), which effects are taken into account in the model, and the elevated input of nutrients caused by anthropogenic activities localized into this part of the Gulf of Sirte.

The vertical chlorophyll profiles obtained by the 3D model close to the hydrological stations were compared to the corresponding experimental profiles collected during the MedSudMed-08 oceanographic survey (see Figs. 2-4). The comparison was performed only in hydrological stations (36 over 42) where the bathymetry was greater than 2.5 m depth, while the rest of the stations (6 over 42) were excluded due to both insignificant water column depth (approximately 0 m) and the selected spatial resolution.

From a qualitative point of view, the theoretical chlorophyll profiles (blue line) agree with observed experimental profiles (red line) in most of the 36 analysed hydrological stations.

According to the Chi square test all the selected stations showed not significant differences between simulated and measured chlorophyll values (Table 2). Further, the K-S test comparing also the shape of the chlorophyll profiles suggested that the null hypothesis can be accepted for twenty-eight hydrological station at 95% of probability (α=0.05), five at 99% (α=0.01) and three hydrological stations at 99,9% (α=0.001). The statistical tests indicated a poor agreement between theoretical results and experimental data only in eight hydrological stations. Here, the differences were statistically significant with a P-value of less than 0.01. In particular, we observe that the closer we get to the Libyan coast, the more statistically significant the difference and the lower the P-value. In fact, most of the statistically different hydrological stations were located in the neighbouring coastal region. More specifically, most of these stations were found in the western part of the domain (see Table 2 and Figs. 2-4). These statistical differences observed in hydrological stations close to the coast were probably due to the higher presence of phytoplankton groups (>3 μm), such as diatoms, not considered in this modeling approach. Different authors have confirmed the significant presence of diatoms in coastal area of the Mediterranean Sea [73, 74]. On the other hand, Brunet et al. [52, 69] indicated that diatoms have a minor presence in off shore area in the Strait of Sicily.

4. Discussion

In this work, we have introduced an innovative approach to investigate the spatio-temporal dynamics of phytoplankton in marine environments that are too difficult to experimentally explore due to security concerns and geo-political problems. Compared to previous works [5, 6, 29, 34, 38], the advection-diffusion-reaction 3D model took into account the experimental data both on the velocity field of sea currents and on the nutrient concentration, acquired in the Gulf of Sirte during the MedSudMed-08 oceanographic survey. It is worth noting that the experimental velocity fields and nutrient concentrations, used as input in the model, are totally independent and uncorrelated from the experimental phytoplankton concentrations acquired in the MedSudMed-08 oceanographic survey.

This makes statistically correct and significative the comparison between the two spatio-temporal phytoplankton distributions, i.e., the one obtained from the model, the other consisting of field data. In particular, the model exploited the hydrological and chemical variables experimentally measured to set the initial and boundary conditions in the investigated 3D domain. Moreover, the 3D model was integrated with satellite remote sensing data, through which it took into account the daily temporal variations in the intensity of the incident light. In particular, the data set of Surface meteorology and Solar Energy (SSE) obtained from various satellite platforms of NASA and NOAA, allowed the integration of light intensity data on a daily basis and for the whole model run period. All these modifications were used to improve the modeling of the dynamics of phytoplankton abundance and chlorophyll concentration. In this way, the model provided important insights into the role of physical and biological environmental variables in the formation of phytoplankton biomass, which is the lowest level of the food chain in marine ecosystems. In the proposed model, environmental conditions were set based on experimental on-field observations. In particular, both the three-dimensional distribution of the concentration of nutrients of the domain and the velocity field of marine currents at the steady state were obtained by interpolating the experimental data collected in forty-two hydrological stations of the Gulf of Sirte during the MedSudMed-08 oceanographic survey (see Supplementary Information). Conversely, the horizontal and vertical turbulent diffusivities have been fixed constant for the entire 3D domain, in accordance with environmental conditions observed experimentally [29, 34]. Subsequently, the 3D model equations were solved to reproduce the spatio-temporal behaviour of phytoplankton abundance for the four investigated populations, considering the competition for growth limiting factors, i.e., light intensity and nutrient concentration. The coexistence of the four phytoplankton populations considered was ensured by setting the biological parameters in accordance with previous experimental observations [52, 75, 76, 77]. Then, the phytoplankton abundances were converted into theoretical concentrations of *chl-a* and *Dvchl-a* using the conversion curves obtained in previous works [52, 69]. The theoretical results for the total chlorophyll concentration were compared with the corresponding experimental data acquired on the hydrological stations considered. The model results were tested quantitatively by statistical tests (Chi-squared and Kolmogorov-Smirnov). From a qualitative point of view, the model results indicated that the spatial distribution of the *chl-a* concentration strongly depends on the velocity field of sea currents and vertical turbulent diffusivity, both of which could change significantly in next few years due to the global warming, modifying the food web of the Gulf of Sirte. Specifically, an increase in seawater temperature in shallower layers of the water column could cause a strong decrease in vertical turbulent diffusivity, which would determine the permanence of DCM in deeper layers even during the winter season with catastrophic effects for pelagic fish living the investigated area [78, 79]. Furthermore, significant modifications in the regime of marine currents could occur at the surface layer of the water column, causing significant changes in the horizontal distribution of the *chl-a* concentration. The model results also showed that the depth, width and magnitude of DCM depend on biological parameters, which were set to the same values for all sites according to the homogenous environmental conditions observed in the Gulf of Sirte. Unlike the 2D model devised for the Cape Passero-Misurata transect [34], here setting the values of half-saturation constants at the same values for the whole domain to ensure a good agreement between theoretical results and experimental data in most of the hydrological stations. These findings demonstrate that our three-dimensional model reproduces, in homogeneous environments, the spatial distribution of *chl-a* concentration better than the one- and two-dimensional models. Overall, the quantitative comparison showed that the 3D model successfully simulated the spatial distribution of chlorophyll concentration in most of the Gulf of Sirte. In particular, the statistical analysis indicated a good agreement between the theoretical and experimental chlorophyll profiles at around 80 % of the stations investigated in this work. Meanwhile, a poor agreement between the theoretical and experimental chlorophyll profiles was observed in few hydrological stations (eight out of thirty-six), most of these stations were located near the Libyan shore. Probably, this behaviour is due to the increased presence of nano- and micro- phytoplankton groups (>3 μm), such as diatoms, which are not considered directly in this model. Regarding

phytoplankton assemblages and the vertical distribution of phytoplankton communities, it has been noticed that picophytoplankton dominated in terms of chlorophyll concentration throughout the euphotic zone. Specifically, Synechococcus was localized in the surface layer, Prochlorococcus HL was present in the surface and intermediate layers (0-100 m), while Prochlorococcus LL and picoeukaryotes were mainly present in the deeper layers of the water column. Furthermore, Prochlorococcus LL largely dominated the other groups of picophytoplankton in deep environment with limited light. Finally, the results indicate that light/nutrient requirements are the major drivers of phytoplankton dynamics in the Gulf of Sirte.

Overall, the study indicates that the proposed three-dimensional advection-diffusion-reaction model can provide reliable data on the spatio-temporal dynamics of chlorophyll concentration in marine environments. Moreover, the modeling approach developed here provides a powerful resource for further theoretical investigations that can deepen our knowledge on the dynamics of chlorophyll concentration and phytoplankton abundances. In particular, further improvements can be obtained by incorporating: (i) marine circulation models as a direct approach to take into account the spatio-temporal dynamics of marine currents and the horizontal and vertical turbulent diffusivities; (ii) the contribution of the chlorophyll of larger diatoms to the total chlorophyll concentration, particularly in coastal areas; iii) the role of random environmental fluctuations modeled through multiplicative noise sources. Indeed, the constructive role of environmental noise has been observed and modeled in a plethora of physical and biological systems, including also financial ones [80, 81, 82, 83, 84].

Moreover, the presence of these multiplicative noise sources, which act on the dynamics of phytoplankton populations and nutrient, can allow to further improve the agreement between theoretical results and experimental findings, as observed in 1D models (see ref. [6] and references therein). One of the main reasons of the discrepancies between theoretical and experimental *chlorophyll a* distributions can be ascribed to the use of deterministic reaction-diffusion-taxis models [5], in which the nutrient half-saturation coefficients are assumed to be constant during the whole year. On the contrary, stochastic models take into account the continuous changes due to environmental random fluctuations [6], which affect both biological and physical variables, and provide therefore a more realistic description of the ecosystem dynamics.

As a final observation we wish to underline that the application and validation of this model in a distant and relatively politically unstable area can be an efficient tool to replace experimental measures when the area cannot be explored for political and security reasons. Such a modeling approach can overcome the spatio-temporal limitations of sampling coverage, can be applied in remote region regardless from weather conditions and can limit the need for expensive oceanographic surveys. In particular, the modeling approach allows periodic monitoring of chlorophyll dynamics and the structure of the phytoplankton community in ecosystems that are difficult to access such as the Gulf of Sirte. Finally, we recall that such a model could be essential for understanding and predicting the effects of global warming on phytoplankton dynamics and primary production in marine ecosystems and therefore for ecosystem-based assessment models of fishery. Rather than climatic importance as a biological carbon pump, phytoplankton are primary producers, their modeling can be invaluable in assessing the abundancies of other species and even the whole aquatic food web.

References

[1] P. G. Falkowski, R. T. Barber and V. Smetacek, "Biogeochemical controls and feedbacks on ocean primary production.," *Science,* vol. 281, no. 5374, pp. 200-206, 1998.

[2] D. Righetti, M. Vogt, N. Gruber, A. Psomas and N. E. Zimmermann, "Global pattern of phytoplankton diversity driven by temperature and environmental variability.," *Science advances,* vol. 5, no. (5), p. eaau6253, 2019.

[3] C. B. Field, M. J. Behrenfeld, J. T. Randerson and P. Falkowski, "Primary production of the biosphere: integrating terrestrial and oceanic components.," *Science,* vol. 281, no. 5374, pp. 237-240, 1998.

[4] R. El Hourany, M. Abboud-Abi Saab, G. Faour, O. Aumont, M. Crépon and S. Thiria, "Phytoplankton Diversity in the Mediterranean Sea from satellite data using self-organizing maps.," *J. Geophys. Res. Oceans,* vol. 124, pp. 5827-5843, 2019.

[5] D. Valenti, G. Denaro, B. Spagnolo, F. Conversano and C. Brunet, "How diffusivity, thermocline and incident light intensity modulate the dynamics of deep chlorophyll maximum in Tyrrhenian Sea.," *PLoS ONE,* vol. 10, no. 1, p. e0115468, 2015.

[6] D. Valenti, G. Denaro, B. Spagnolo, S. Mazzola, G. Basilone, F. Conversano, C. Brunet and A. Bonanno, "Stochastic models for phytoplankton dynamics in Mediterranean Sea.," *Ecol. Complex.,* vol. 27, p. 84–103, 2016.

[7] G. Basilone, S. Mangano, M. Pulizzi, I. Fontana, G. Giacalone, R. Ferreri, A. Gargano, S. Aronica, M. Barra, S. Genovese, P. Rumolo, S. Mazzola and A. Bonanno, "European anchovy (Engraulis encrasicolus) age structure and growth rate in two contrasted areas of the Mediterranean Sea: the paradox of faster growth in oligotrophic seas," *Mediterr. Mar. Sci.,* vol. 18, no. 3, pp. 504-516, 2017.

[8] A. Bonanno, M. Barra, R. Mifsud, G. Basilone, S. Genovese, M. Di Bitetto, S. Aronica, G. Giacalone, I. Fontana, S. Mangano, R. Ferreri, M. Pulizzi, P. Rumolo, A. Gargano, G. Buscaino, P. Calandrino, A. Di Maria and S. Mazzola, "Space utilization by key species of the pelagic fish community in an upwelling ecosystem of the Mediterranean Sea.," *Hydrobiologia,* vol. 821, no. 1, pp. 173-190, 2018.

[9] A. Bonanno, S. Zgozi, G. Basilone, M. Hamza, M. Barra, S. Genovese, P. Rumolo, A. Nfate, M. Elsger, S. Goncharov, S. Popov, R. Mifsud, T. Bahri, G. Giacalone, I. Fontana, B. Buongiorno Nardelli, S. Aronica, B. Patti, Giac and L. Ceriola, "Acoustically detected pelagic fish community in relation to environmental conditions observed in the Central Mediterranean Sea: a comparison of Libyan and Sicilian–Maltese coastal areas.," *Hydrobiologia,* vol. 755, no. Issue 1, pp. 209-224, 2015.

[10] A. Bonanno, M. Barra, G. Basilone, S. Genovese, P. Rumolo, S. Goncharov, S. Popov, B. Buongiorno Nardelli, D. Iudicone, G. Procaccini, S. Aronica, B. Patti, G. Giacalone, R. Ferreri, I. Fontana, G. Tranchida, S. Mangano, M. Pulizzi and Garga, "Environmental processes driving anchovy and sardine distribution in a highly variable environment: the role of the coastal structure and riverine input.," *Fish. Oceanogr.,* vol. 25, no. 5, pp. 471-490, 2016.

[11] G. H. Krause and E. Weis, "Chlorophyll fluorescence and photosynthesis: the basics.," *Annu. Rev. Plant Physiol. Plant Mol. Biol.,* vol. 42, pp. 313-349, 1991.

[12] R. G. Williams and M. L. Follows, Ocean dynamics and the carbon cycle: Principles and Mechanisms., Cambridge University Press, 2011.

[13] G. C. Hays, A. J. Richardson and C. Robinson, "Climate change and marine plankton.," *Trends Ecol. Evol.,* vol. 20, no. 6, pp. 337-344, 2005.

[14] R. Cavicchioli, W. J. Ripple, K. N. Timmis, F. Azam, L. R. Bakken, M. Baylis, M. J. Behrenfeld, A. Boetius, P. W. Boyd, A. T. Classen, T. W. Crowther, R. Danovaro, C. M. Foreman, J. Huisman, D. A. Hutchins, J. K. Jansson, D. M. Karl and Kosk, "Scientists' warning to humanity: microorganisms and climate change.," *Nat. Rev. Microbiol.,* vol. 17, pp. 569-586, 2019.

[15] T. O. Fossum, G. M. Fragoso, E. J. Davies, J. E. Ullgren, R. Mendes, G. Johnsen, I. Ellingsen, J. Eidsvik, M. Ludvigsen and K. Rajan, "Toward adaptive robotic sampling of phytoplankton in the coastal ocean.," *Science Robotics,* vol. 4, no. 27, 2019.

[16] P. Falkowski, "Ocean Science: The power of plankton.," *Nature,* vol. 483, pp. S17-S20, 2012.

[17] O. Hoegh-Guldberg and J. F. Bruno, "The impact of climate change on the world's marine ecosystems.," *Science,* vol. 328, no. 5985, pp. 1523-1528, 2010.

[18] T. Wernberg, B. D. Russell, P. J. Moore, S. D. Ling, D. A. Smale, A. Campbell, M. A. Coleman, P. D. Steinberg, G. A. Kendrick and S. D. Connell, "Impacts of climate change in a global hotspot for temperate marine biodiversity and ocean warming.," *J. Exp. Mar. Biol. Ecol.,* vol. 400, pp. 7-16, 2011.

[19] J. P. McCarty, "Ecological consequences of recent climate change.," *Conserv. Biol.,* vol. 15, no. 2, pp. 320-331, 2001.

[20] A. G. Ostrovskii, A. G. Zatsepin, V. A. Soloviev, A. L. Tsibulsky and D. A. Shvoev, "Autonomous system for vertical profiling of the marine environment at a moored station.," *Oceanology,* vol. 53, no. 2, pp. 233-242, 2013.

[21] C. Whitt, J. Pearlman, B. Polagye, F. Caimi, F. Muller-Karger, A. Copping, H. Spence, S. Madhusudhana, W. Kirkwood, L. Grosjean, B. M. Fiaz, S. Singh, D. Manalang, A. S. Gupta, A. Maguer, J. J. H. Buck, A. Marouchos, M. A. Atmanand and Venka, "Future vision for autonomous ocean observations.," *Frontiers in Marine Science,* vol. 7, p. 697, 2020.

[22] C. R. McClain, "A decade of satellite ocean color observations.," *Annu. Rev. Mar. Sci.,* vol. 1, pp. 19-42, 2009.

[23] D. A. Siegel, M. J. Behrenfeld, S. Maritorena, C. R. McClain, D. Antoine, S. W. Bailey, P. S. Bontempi, E. S. Boss, H. M. Dierssen, S. C. Doney, R. E. Eplee, R. H. Evans, G. C. Feldman, E. Fields, B. A. Franz, N. A. Kuring, C. Mengelt and Ne, "Regional to global assessments of phytoplankton dynamics from the SeaWiFS mission.," *Remote Sens. Environ.,* vol. 135, pp. 77-91, 2013.

[24] M. Lévy, P. J. S. Franks and K. S. Smith, "The role of submesoscale currents in structuring marine ecosystems.," *Nat. Commun.,* vol. 9, no. 4758, 2018.

[25] J. Huisman, N. N. P. Thi, D. M. Karl and B. Sommeijer, "Reduced mixing generates oscillations and chaos in the oceanic deep chlorophyll maximum.," *Nature,* vol. 439, pp. 322-325, 2006.

[26] R. J. W. Brewin, N. J. Hardman-Mountford, S. J. Lavender, D. E. Raitsos, T. Hirata, J. Uitz, E. Devred, A. Bricaud, A. Ciotti and B. Gentili, "An intercomparison of bio-optical techniques for detecting dominant phytoplankton size class from satellite remote sensing.," *Remote Sens. Environ.,* vol. 115, no. 2, pp. 325-339, 2011.

[27] H. R. Gordon and W. R. McCluney, "Estimation of the depth of sunlight penetration in the sea for remote sensing.," *Appl. Opt.,* vol. 14, no. 2, pp. 413-416, 1975.

[28] A. Morel and J. F. Berthon, "Surface pigments, algal biomass profiles, and potential production of the euphotic layer: Relationships reinvestigated in view of remote-sensing applications.," *Limnol. Oceanogr.,* vol. 34, no. 8, pp. 1545-1562, 1989.

[29] G. Denaro, D. Valenti, A. La Cognata, B. Spagnolo, A. Bonanno, G. Basilone, S. Mazzola, S. W. Zgozi, S. Aronica and C. Brunet, "Spatio-temporal behaviour of the deep chlorophyll maximum in Mediterranean Sea: Development of a stochastic model for picophytoplankton dynamics.," *Ecol. Complex.,* vol. 13, p. 21–34, 2013.

[30] O. Aumont, C. Éthé, A. Tagliabue, L. Bopp and M. Gehlen, "PISCES-v2: an ocean biogeochemical model for carbon and ecosystem studies.," *Geoscientific Model Development,* vol. 8, no. 8, pp. 2465-2513, 2015.

[31] F. Moullec, N. Barrier, S. Drira, F. Guilhaumon, P. Marsaleix, S. Somot, C. Ulses, L. Velez and Y. J. Shin, "An End-to-End Model Reveals Losers and Winners in a Warming Mediterranean Sea.," *Front. Mar. Sci.,* vol. 6, no. 345, 2019.

[32] J. Greenwood and P. Craig, "A simple numerical model for predicting vertical distribution of phytoplankton on the continental shelf.," *Ecol. Model.,* vol. 273, pp. 165-172, 2014.

[33] N. P. P. Thi, J. Huisman and B. P. Sommeijer, "Simulation of three-dimensional phytoplankton dynamics: competition in light-limited environments.," *J. Comp. Appl. Math.,* vol. 174, pp. 57-77, 2005.

[34] D. Valenti, G. Denaro, R. Ferreri, S. Genovese, S. Aronica, S. Mazzola, A. Bonanno, G. Basilone and B. Spagnolo, "Spatio-temporal dynamics of a planktonic system and chlorophyll distribution in a 2D spatial domain: matching model and data.," *Sci. Rep.,* vol. 7, no. 220, 2017.

[35] D. Valenti, A. Giuffrida, G. Denaro, N. Pizzolato, L. Curcio, S. Mazzola, G. Basilone, S. Aronica, A. Bonanno and B. Spagnolo, "Noise Induced Phenomena in the Dynamics of Two Competing Species.," *Math. Model. Nat. Phenom.,* vol. 11, no. 5, pp. 158-174, 2016.

[36] D. Valenti, G. Denaro, F. Giarratana, A. Giuffrida, S. Mazzola, G. Basilone, S. Aronica, A. Bonanno and B. Spagnolo, "Modeling of Sensory Characteristics Based on the Growth of Food Spoilage Bacteria.," *Math. Model. Nat. Phenom.,* vol. 11, no. 5, pp. 119-136, 2016.

[37] C. A. Klausmeier and E. Litchman, "Algal games: the vertical distribution of phytoplankton in poorly mixed water columns.," *Limnol. Oceanogr.,* vol. 46, p. 1998–2007, 2001.

[38] G. Denaro, D. Valenti, B. Spagnolo, G. Basilone, S. Mazzola, S. W. Zgozi, S. Aronica and A. Bonanno, "Dynamics of two picophytoplankton groups in Mediterranean Sea: Analysis of the deep chlorophyll maximum by a stochastic advection-reaction-diffusion model.," *PloS one,* vol. 8, no. 6, p. e66765, 2013.

[39] G. Denaro, D. Valenti, B. Spagnolo, A. Bonanno, G. Basilone, S. Mazzola, S. W. Zgozi and S. Aronica, "Stochastic dynamics of two picophytoplankton populations in a real marine ecosystem.," *Acta Phys. Pol. B,* vol. 44, p. 977–990, 2013.

[40] D. Valenti, G. Denaro, F. Conversano, C. Brunet, A. Bonanno, G. Basilone, S. Mazzola and B. Spagnolo, "The role of noise on the steady state distributions of phytoplankton populations.," *J. Stat. Mech.,* vol. 2016, no. 5, p. 054044, 2016.

[41] A. Morozov, G. Denaro, B. Spagnolo and D. Valenti, "Revisiting the role top-down and bottom-up controls in stabilisation of nutrient-rich plankton communities.," *Commun. Nonlinear Sci.,* vol. 79, p. 104885, 2019.

[42] G. Bougaran, O. Bernard and A. Sciandra, "Modeling continuous cultures of microalgae colimited by nitrogen and phosphorus.," *J. Theor. Biol.,* vol. 265, no. 3, pp. 443-454, 2010.

[43] S. Diehl, S. A. Berger, R. Ptacnik and A. Wild, "Phytoplankton, light, and nutrients in a gradient of mixing depths: field experiments.," *Ecology,* vol. 83, no. 2, pp. 399-411, 2002.

[44] J. S. Wroblewski and J. J. O'Brien, "A spatial model of phytoplankton patchiness.," *Mar. Biol.,* vol. 35, no. 2, pp. 161-175, 1976.

[45] A. B. Ryabov, L. Rudolf and B. Blasius, "Vertical distribution and composition of phytoplankton under the influence of an upper mixed layer.," *J. Theor. Biol.,* vol. 263, no. (1), pp. 120-133, 2010.

[46] Y. Du and L. Mei, "On a nonlocal reaction–diffusion–advection equation modelling phytoplankton dynamics.," *Nonlinearity,* vol. 24, no. (1), pp. 319-349, 2010.

[47] P. A. Auger, F. Diaz, C. Ulses, C. Estournel, J. Neveux, F. Joux, M. Pujo-Pay and J. J. Naudin, "Functioning of the planktonic ecosystem on the Gulf of Lions shelf (NW Mediterranean) during spring and its impact on the carbon deposition: a field data and 3-D modelling combined approach.," *Biogeosciences,* vol. 8, no. (11), pp. 3231-3261, 2011.

[48] T. Kim and M. Lin, "Stable advection-reaction-diffusion with arbitrary anisotropy," *Comp. Anim. Virtual Worlds,* vol. 18, pp. 329-338, 2007.

[49] P. Grasso and M. S. Innocente, "A two-dimensional reaction-advection-diffusion model of the spread of fire in wildlands," in *Advances in Forest Fire Research*, D.X. Viegas (Ed.), Chapter 3, Fire Management, 2018, pp. pp. 334-342.

[50] N. Emken and C. Engwer, "A reaction-diffusion-advection model for the establishment and maintenance of transport-mediated polarity and symmetry breaking," *Front. Appl. Math Stat.,* vol. 6, no. 570036, 2020.

[51] A. S. Kim, "Complete analytic solutions for convection-diffusion-reaction-source equations without using an inverse Laplace transform," *Sci. Rep.,* vol. 10, no. 8040, 2020.

[52] C. Brunet, R. Cassotti, V. Vantrepotte and F. Conversano, "Vertical variability and diel dynamics of picophytoplankton in the Strait of Sicily, Mediterranean Sea, in summer.," *Mar. Ecol. Prog. Ser.,* vol. 346, p. 15–26, 2007.

[53] F. Placenti, K. Schroeder, A. Bonanno, S. Zgozi, M. Sprovieri, M. Borghini, P. Rumolo, G. Cerrati, S. Bonomo, S. Genovese, G. Basilone, D. A. Haddoud, B. Patti, A. El Turki, M. Hamza and S. Mazzola, "Water masses and nutrient distribution in the Gulf of Syrte and between Sicily and Libya.," *J. Marine Syst.,* vol. 121–122, p. 36–46, 2013.

[54] A. Bonanno, F. Placenti, G. Basilone, R. Mifsud, S. Genovese, B. Patti, M. Di Bitetto, S. Aronica, M. Barra, G. Giacalone, R. Ferreri, I. Fontana, G. Buscaino, G. Tranchida, E. Quinci and S. Mazzola, "Variability of water mass properties in the Strait of Sicily in summer period of 1998–2013.," *Ocean Sci.,* vol. 10, p. 1–12, 2014.

[55] M. Visbeck, "Deep velocity profiling using lowered acoustic Doppler current profiers: bottom track and inverse solutions.," *J. Atmos. Ocean. Technol.,* vol. 19, no. (5), p. 794–807, 2002.

[56] M. Quevedo and R. Anadón, "Protist control of phytoplankton growth in the subtropical north-east Atlantic.," *Mar. Ecol. Prog. Ser.,* vol. 221, p. 20–38, 2001.

[57] J. A. Raven, "The twelfth Tansley lecture. Small is beautiful: the picophytoplankton.," *Funct. Ecol.,* vol. 12, p. 503–513, 1998.

[58] J. A. Raven, Z. V. Finkel and A. J. Irwin, "Picophytoplankton: bottom-up and top-down controls on ecology and evolution.," *J. Geophys. Res.,* vol. 55, p. 209–215, 2005.

[59] D. H. Turpin, in *Physiological mechanisms in phytoplankton resource competition. In: Growth and reproductive strategies of freshwater phytoplankton.*, Cambridge University Press, 1988, p. 316–368.

[60] C. A. Klausmeier, E. Litchman and S. A. Levin, "A model of flexible uptake of two essential resources.," *J. Theor. Biol.,* vol. 246, pp. 278-289, 2007.

[61] M. Ribera d'Alcalà, G. Civitarese, F. Conversano and R. Lavezza, "Nutrient ratios and fluxes hint at overlooked processes in the Mediterranean Sea.," *J. Geophys. Res.,* vol. 108, no. (C9), p. 8106, 2003.

[62] R. C. Pacanowski and S. G. H. Philander, "Parameterization of Vertical Mixing in Numerical Models of Tropical Oceans.," *J. Phys. Oceanogr.,* vol. 11, p. 1443–1451, 1981.

[63] S. R. Massel, Fluid Mechanics for Marine Ecologists, 1999: Springer-Verlag, Berlin Heidelberg.

[64] N. Shigesada and A. Okubo, "Effcts of competition and shading in planktonic communities.," *J. Math. Biol.,* vol. 12, p. 311–326, 1981.

[65] J. T. O. Kirk, Light and Photosynthesis in Aquatic Ecosystems (2nd edition), Cambridge University Press, 1994.

[66] W. Hundsdorfer and J. G. Verwer, Numerical solution of time-dependent advection-diffusion-reaction equations., Berlin: Springer-Verlag, 2003.

[67] M. Dehghan, "Numerical solution of the three-dimensional advection–diffusion equation.," *Appl. Math. Comput.,* vol. 150, pp. 5-19, 2004.

[68] A. Morel, Y. H. Ahn, F. Partennsky, D. Vaulot and H. Claustre, "Prochlorococcus and Synechococcus: A comparative study of their optical properties in relation to their size and pigmentation.," *J. Mar. Res.,* vol. 51, pp. 617-649, 1993.

[69] C. Brunet, R. Casotti, V. Vantrepotte, F. Corato and F. Conversano, "Picophytoplankton diversity and photoacclimation in the Strait of Sicily (Mediterranean Sea) in summer. I. Mesoscale variations.," *Aquat. Microb. Ecol.,* vol. 44, pp. 127-141, 2006.

[70] R. Casotti, A. Landolfi, C. Brunet, F. D'Ortenzio, O. Mangoni, M. Ribera d'Alcalà and M. Denis, "Composition and dynamics of the phytoplankton of the Ionian Sea (eastern Mediterranean).," *J. Geophys. Res. Oceans,* vol. 108, no. (C9), p. 8116, 2003.

[71] T. Yogev, E. Rahav, E. Bar-Zeev, D. Man-Aharonovich, N. Stambler, N. Kress, O. Béjà, M. R. Mulholland, B. Herut and I. Berman-Frank, "Is dinitrogen fixation significant in the Levantine Basin, East Mediterranean Sea?," *Environ. Microbiol.,* vol. 13, no. (4), pp. 854-871, 2011.

[72] C. Mena, P. Reglero, M. Hidalgo, E. Sintes, R. Santiago, M. Martin, G. Moyà and R. Balbin, "Phytoplankton community structure is driven by stratification in the oligotrophic Mediterranean Sea.," *Front. Microbiol.,* vol. 10, p. 1698, 2019.

[73] C. Brunet, R. Chandrasekaran, L. Barra, V. Giovagnetti, F. Corato and A. V. Ruban, "Spectral radiation dependent photoprotective mechanism in the diatom pseudo-nitzschia multistriata," *Plose One,* vol. 9, no. Issue 1, p. e87015, 2014.

[74] V. Giovagnetti, S. Flori, F. Tramontano, J. Lavaud and C. Brunet, "The velocity of light intensity increase modulates the photoprotective response in coastal diatoms.," *Plose One,* vol. 9, no. Issue 8, p. e103782, 2014.

[75] S. Bertilsson, O. Berglund, D. M. Karl and S. W. Chisholm, "Elemental composition of marine Prochlorococcus and Synechococcus: implications for the ecological stoichiometry of the sea.," *Limnol. Oceanogr.,* vol. 48, p. 1721–1731, 2003.

[76] K. R. Timmermans, B. van der Wagt, M. J. W. Veldhuis, A. Maatman and H. J. W. de Baar, "Physiological responses of three species of marine pico-phytoplankton to ammonium, phospahte, iron and light limitation.," *J. Sea Res.,* vol. 53, p. 109–120, 2005.

[77] M. J. W. Veldhuis, K. R. Timmermans, P. Croot and B. Van Der Wagt, "Picophytoplankton; a comparative study of their biochemical composition and photosynthetic properties.," *J. Sea Res.,* vol. 53, p. 7–24, 2005.

[78] J. A. Gittings, D. E. Raitsos, G. Krokos and I. Hoteit, "Impacts of warming on phytoplankton abundance and phenology in a typical tropical marine ecosystem.," *Scientific reports,* vol. 8, no. (1), pp. 1-12, 2018.

[79] S. C. Doney, "Oceanography: Plankton in a warmer world.," *Nature,* vol. 444, no. (7120), p. 695–696, 2006.

[80] B. Spagnolo and D. Valenti, "Volatility effects on the escape time in financial market models," *Int. J. Bifurcation and Chaos,* vol. 18, pp. 2775-2786, 2008.

[81] A. Giuffrida, D. Valenti, G. Ziino, B. Spagnolo and A. Panebianco, "A stochastic interspecific competition model to predict the behaviour of Listeria monocytogenes in the fermentetion process of a traditional Sicilian salami," *Eur. Food Res. Technol.,* vol. 228, pp. 767-775, 2009.

[82] N. Pizzolato, A. Fiasconaro, D. Perano Adorno and D. Spagnolo, "Resonant activation in polymer translocation: new insights into the escape dynamics of molecules driven by an oscillating field," *Phys. Biol.,* vol. 7, no. 034001, 2010.

[83] C. Guarcello, D. Valenti, A. Carollo and B. Spagnolo, "Effects of Lévy noise on the dynamics of sine-Gordon solitons in long Josephson junctions," *J. Stat. Mech. Theory E.,* vol. 2016, 2016.

[84] A. Carollo, B. Spagnolo and D. Valenti, "Uhlmann curvature in dissipative phase transitions," *Sci. Rep.,* vol. 8, no. 9852, 2018.

[85] B. B. Jørgensen and A. Boetius, "Feast and famine-microbial life in the deep-sea bed.," *Nat. Microbiol. Rev.,* vol. 5, pp. 770-781, 2007.

[86] C. Brunet, R. Casotti and V. Vantrepotte, "Phytoplankton diel and vertical variability in photobiological responses at a coastal station in the Mediterranean Sea.," *J. Plankton Res.,* vol. 30, pp. 645-654, 2008.

[87] L. Garczarek, A. Dufresne, S. Rousvoal, N. J. West, S. Mazard, D. Marie, H. Claustre, P. Raimbault, A. F. Post, D. J. Scanlan and F. Partensky, "High vertical and low horizontal diversity of Prochlorococcus ecotypes in the Mediterranean Sea in summer.," *FEMS Microbiol. Ecol.,* vol. 60, pp. 189-206, 2007.

[88] D. Valenti, G. Denaro, A. La Cognata, B. Spagnolo, A. Bonanno, G. Basilone, S. Mazzola, S. Zgozi and S. Aronica, "Picophytoplankton dynamics in noisy marine environment.," *Acta Phys. Pol. B,* vol. 43, p. 1227–1240, 2012.

[89] T. F. Thingstad and E. Sakshaugh, "Control of phytoplankton growth in nutrient recycling ecosystems. Theory and terminology.," *Mar. Ecol. Prog. Ser.,* vol. 63, p. 261–272, 1990.

1
2
3
4

Acknowledgments

Special thanks go to all the people and all the authorities who in various ways believed and helped and contributed in a diplomatic, political and military way to the realization of the survey. Moreover, we would thank Dr. Gianpietro Gasparini for his supervision in the survey design and data processing; Mr. Nurredin Essarbout (MBRC, Libya) is thanked for the efforts and support he provided the organization for all activities; Mr. Emanuele Gentile, Master of the R/V Urania, and all his crew are thanked for their work. All participating institutes and scientists who were on board are gratefully acknowledged for their involvement in the work carried out. **Funding:** This study was supported by: The FAO Project MedSudMed “Assessment and Monitoring of the Fishery Resources and the Ecosystems in the Straits of Sicily”, funded by the Italian Ministry MIPAAF. The BLU-DATA-BIO Project "Experts in Hydro-acoustics, Data Analysis, ICT and Protection of Marine Biodiversity" Funding: PO FES Sicily 2014-2020, supported one of the authors of this study allowing him to deepen the specific research topic. **Author contributions:** RF, SG, SA, SM, AB, SZ, GB conceived and designed the experiments; RF, SG, SA, AB, GB, SZ, GG, IF performed the experiments; HA, SA, DV, GD developed the numerical models; HA, SA, GD, GB analysed the data and interpreted results; HA, SA, GD wrote the paper; HA, SA, GD, GB, DV, AB, BS, SM substantively revised the manuscript. **Competing interests:** Authors declare that they have no competing interests. **Data and materials availability:** All data needed to evaluate the conclusions in the paper are present in the main text and the Supplementary Materials. The code and data used in this study are available upon request from the authors.

Figures and Tables

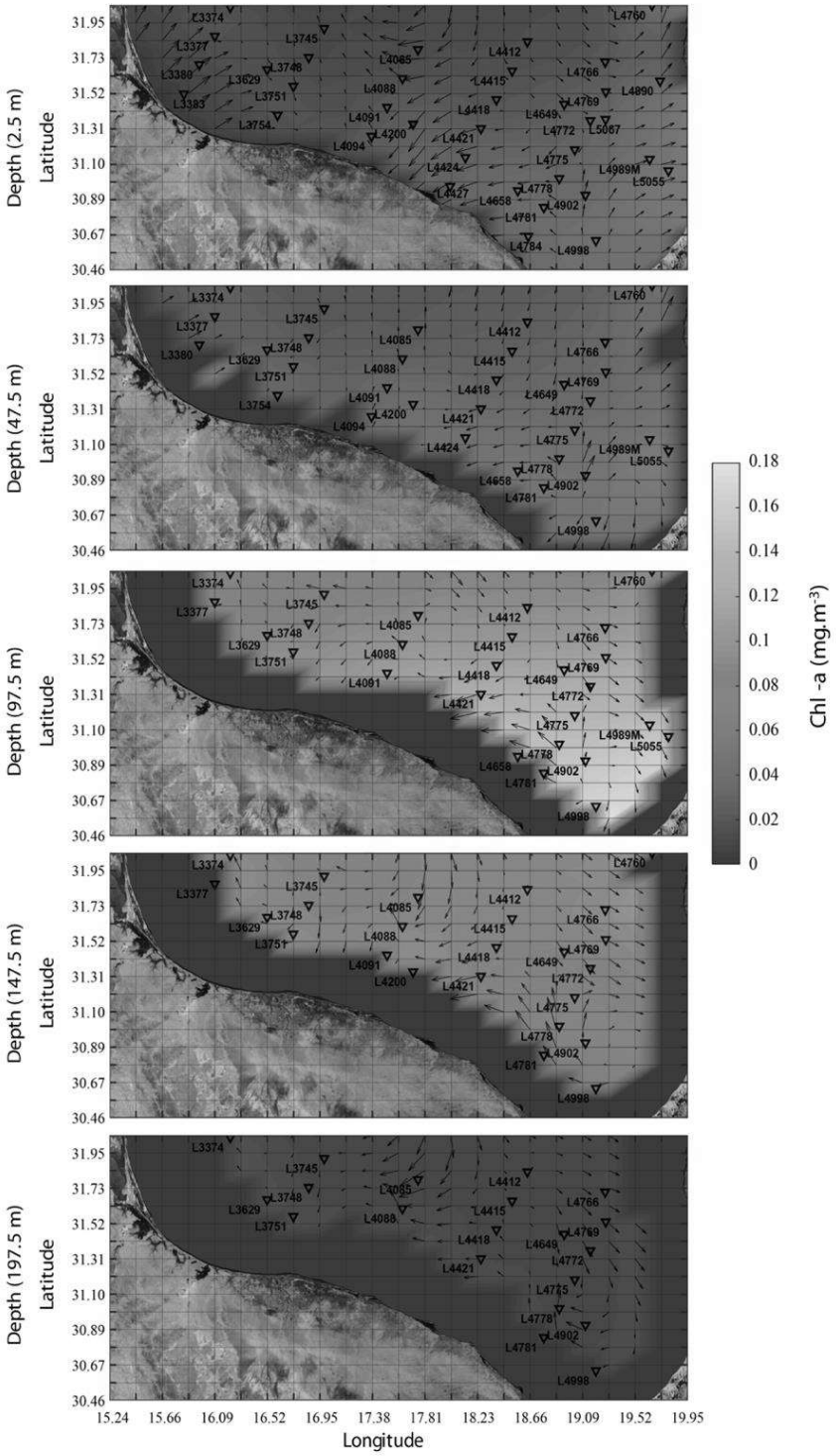

Fig. 1. Horizontal distributions of the total chl-a and Dvchl-a concentration (mg·m^{-3}). The horizontal distributions were obtained by the 3D model for five depth levels (2.5, 47.5, 97.5, 147.5 and 197.5 m). The current vectors were obtained by interpolating the two horizontal components of velocity field, experimentally acquired during the MedSudMed-08 oceanographic survey.

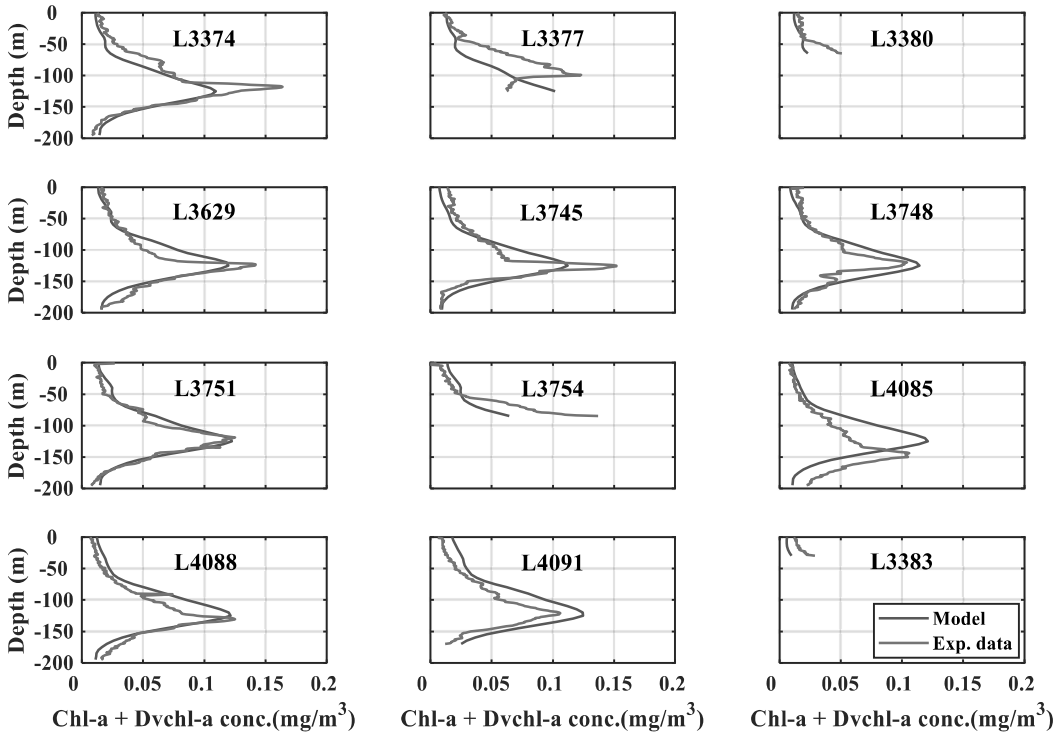

Fig. 2. Theoretical distributions and experimental profiles of the total *chl-a* and *Dvchl-a* concentration. The numerical results (blue line), obtained by the 3D model, are compared with the experimental data (red line) collected in twelve hydrological stations (L3374, L3377, L3380, L3629, L3745, L3748, L3751, L3754, L4085, L4088, L4091 and L3383) of the Gulf of Sirte during the MedSudMed-08 oceanographic survey (15-30 July 2008).

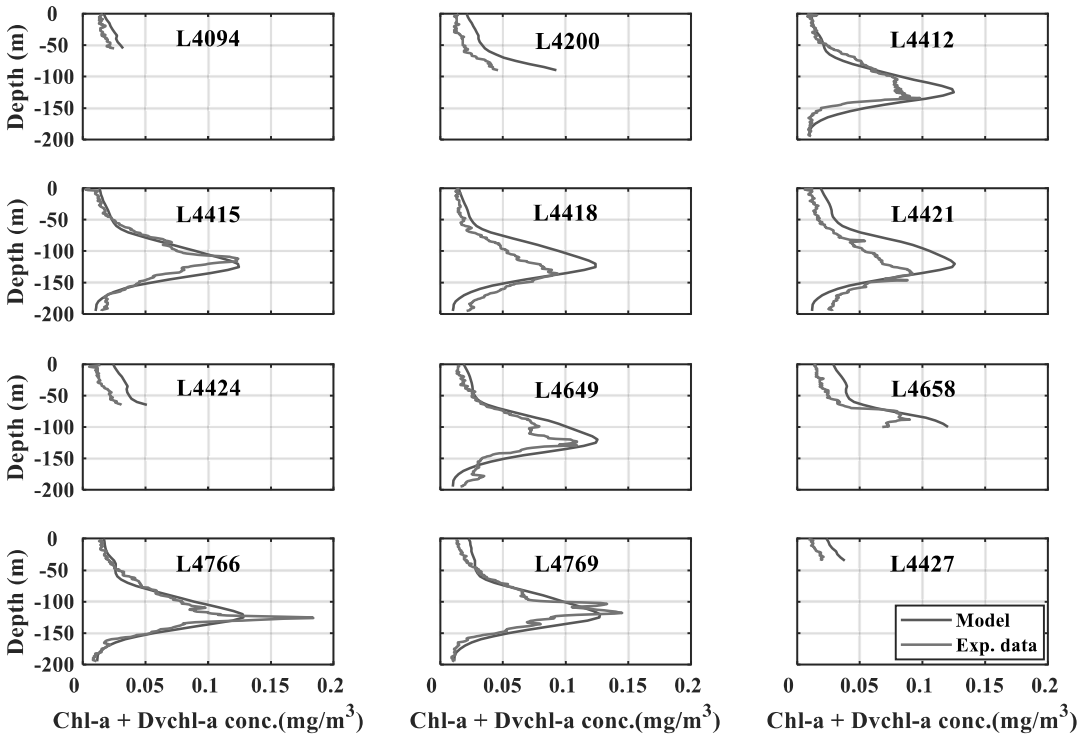

Fig. 3. Theoretical distributions and experimental profiles of the total *chl-a* and *Dvchl-a* concentration. The numerical results (blue line), obtained by the 3D model, are compared with the experimental data (red line) collected in twelve hydrological stations (L4094, L4200, L4412, L4415, L4418, L4421, L4424, L4649, L4658,

L4766, L4769 and L4427) of the Gulf of Sirte during the MedSudMed-08 oceanographic survey (15-30 July 2008).

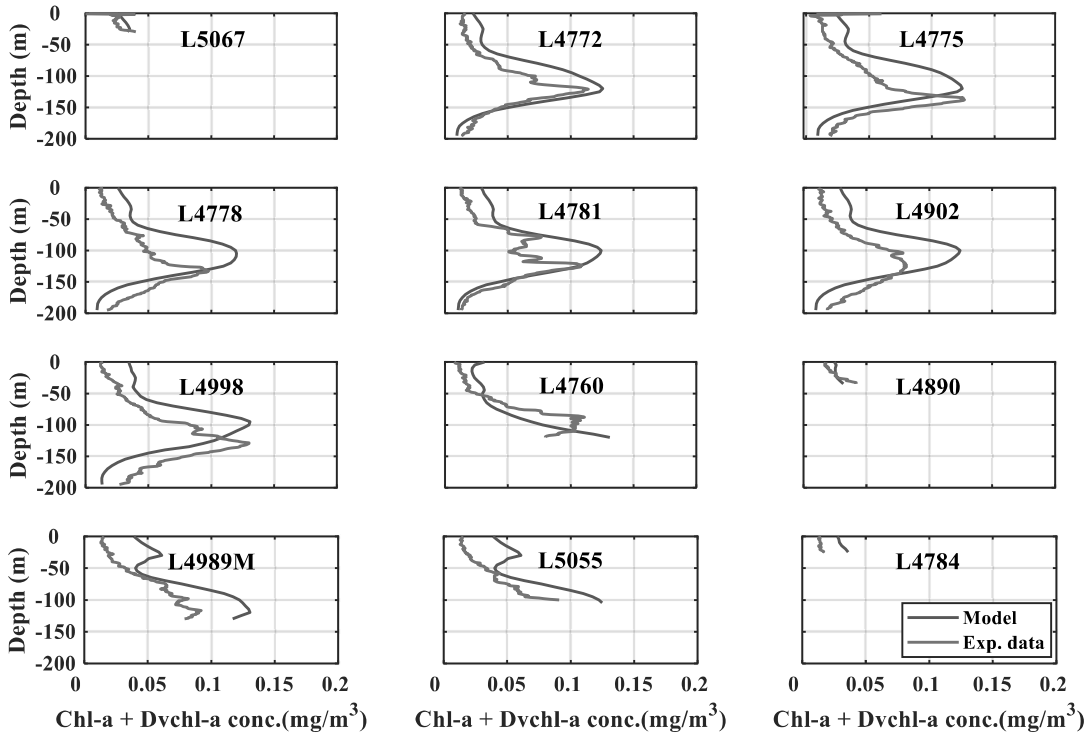

Fig. 4. Theoretical distributions and experimental profiles of the total *chl-a* and *Dvchl-a* concentration. The numerical results (blue line), obtained by the 3D model, are compared with the experimental data (red line) collected in twelve hydrological stations (L5067, L4772, L4775, L4778, L4781, L4902, L4998, L4760, L4890, L4989M, L5055 and L4784) of the Gulf of Sirte during the MedSudMed-08 oceanographic survey (15-30 July 2008).

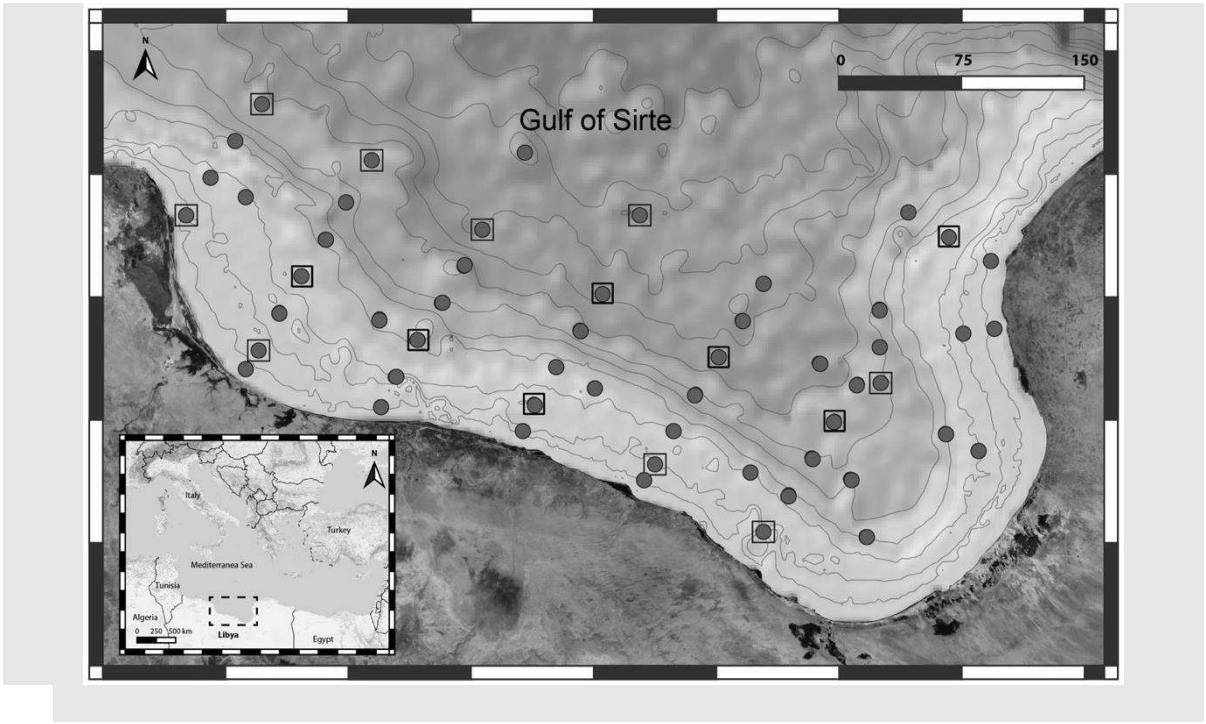

Fig. 5. Geographic location of the Gulf of Sirte in the Libyan coast, Mediterranean Sea. On the right is shown the Gulf of Sirte with the 56 CTD stations (red circles) and the 16 nutrients stations (empty squares) investigated during the MedSudMed-08 oceanographic survey. The bathymetric underlay and bathymetric contours shown on the right were obtained from the General Bathymetric Chart of the Oceans (GEBCO) web portal (https://www.gebco.net).

	0-50 m	50-100 m	100-150 m	150-200 m
Synechococcus	43.95 %	6.54 %	0.04 %	0.00%
Prochlorococcus HL	15.96 %	15.16 %	1.28 %	0.21 %
Picoeukaryotes	5.97 %	31.21 %	16.57 %	15.16 %
Prochlorococcus LL	11.44 %	38.35 %	77.51 %	63.97 %
Tot. picophytoplankton	77.32%	91.17%	95.39%	79.34%

Table 1. Chlorophyll distribution. The chlorophyll is reported in % and is associated to picophytoplankton populations in four different depth layers (0-50, 50-100, 100-150 and 150-200 m).

Station name	*Chi-Square Test*			*Kolmogorov-Smirnov Test*		
	df	χ^2	*Statistical significance*	*D*	*p-value*	*Statistical significance*
L3374	*39*	0,197	ns	0,100	p > .10	ns
L3377	25	0,531	ns	0,269	p > .10	ns
L3380	*13*	0,108	ns	0,429	p > .10	ns
L3383	*6*	0,112	ns	1,000	p < .005	**
L3629	*39*	0,134	ns	0,125	p > .10	ns
L3745	*39*	0,153	ns	0,175	p > .10	ns
L3748	*39*	0,144	ns	0,225	p > .10	ns
L3751	*39*	0,056	ns	0,050	p > .10	ns
L3754	*17*	0,260	ns	0,222	p > .10	ns
L4085	*39*	0,574	ns	0,100	p > .10	ns
L4088	*39*	0,158	ns	0,050	p > .10	ns
L4091	*34*	0,205	ns	0,000	p > .10	ns
L4094	*11*	0,030	ns	0,000	p < .05	*
L4200	*18*	0,175	ns	0,000	p < .001	***
L4412	*39*	0,187	ns	0,025	p > .10	ns
L4415	*39*	0,098	ns	0,050	p > .10	ns
L4418	*39*	0,353	ns	0,075	p > .10	ns
L4421	*39*	0,445	ns	0,000	p > .10	ns
L4424	*13*	0,120	ns	0,000	p < .001	***
L4427	*7*	0,059	ns	0,000	p < .001	***
L4649	*39*	0,198	ns	0,100	p > .10	ns
L4658	*20*	0,166	ns	0,000	p < .005	**
L4766	*39*	0,074	ns	0,075	p > .10	ns
L4769	*39*	0,105	ns	0,050	p > .10	ns
L5067	*6*	0,035	ns	0,143	p < .10	ns
L4772	*39*	0,277	ns	0,100	p < .10	ns
L4775	*39*	0,688	ns	0,075	p > .10	ns
L4778	*39*	0,694	ns	0,100	p > .10	ns
L4781	*39*	0,320	ns	0,100	p < .10	ns
L4784	*5*	0,056	ns	0,000	p < .005	**
L4902	*39*	0,625	ns	0,100	p < .10	ns
L4998	*39*	0,841	ns	0,050	p > .10	ns
L4760	*24*	0,212	ns	0,160	p < .05	*
L4890	*7*	0,011	ns	0,250	p > .10	ns
L4989M	*26*	0,370	ns	0,000	p < .01	**
L5055	*21*	0,313	ns	0,045	p < .005	**

ns = not significant *p<0.05 *p<0.05 **p<0.01 *** p<0.001

Table 2. Results of the statistical analysis in the 36 hydrological stations. The P-value describes the probability value of the difference between the simulated and experimental data, df is the degree of freedom.

Supplementary Materials for

A novel method to simulate the 3-D chlorophyll distribution in marine oligotrophic waters.

H. Awada, S. Aronica*, A. Bonanno, G. Basilone, S. W. Zgozi, G. Giacalone, I. Fontana, S. Genovese, R. Ferreri, S. Mazzola, B. Spagnolo, D. Valenti, G. Denaro

*Corresponding author. Email: salvatore.aronica@cnr.it

Spatial and temporal discretization

Numerical integration of partial differential equations (PDEs) is performed using the method of lines (MOL). In particular, this method discretizes the spatial and temporal domains separately [52]. The MOL approach is useful for addressing various complicated discretization for three-dimensional advection-diffusion models in which the non-linear reaction terms are also present. Numerical analysis of the model was based on an explicit finite difference method forward in time and centred in space (FTCS) for the diffusion terms, and a first-order upwind-biased finite difference scheme for the advection term. The numerical domain involved spatial discretization on a lattice consisting of a rectangular grid of 368 cells for each of the 40 vertical levels. The lattice was defined to cover a computational domain similar to the physical domain representing the Gulf of Sirte (see Figure S1). In particular, the horizontal grid (x- and y-axis) consisted of 23x16 cells with a spatial resolution of 23.335 km along the x-axis from the western to the eastern shore of the Gulf of Sirte, and with a spatial resolution of 13.519 km along the y-axis from Libyan shore at the sea open boundary. The vertical axis (z-axis) included the euphotic layer of the water column from the sea surface to the seabed, and was set to have a maximum depth of 200 m from the sea surface (see Figure S2).
The euphotic layer represents the zone in which phytoplankton populations grow as here they can use the solar energy for making *chlorophyll a* [85]. The period investigated by the model was set at 2 years with a timestep (ΔT) of 10 min. The spatial discretization and the time step have been set to meet the stability criterion according to previous works [33, 66, 67]. The lattice was also designed to set boundaries for data interpolation. In particular, the input matrices of the model were obtained by performing, for each of 40 depth levels, the two-dimensional kriging interpolating of scattered experimental data over the 368 cells of horizontal grid.

Phytoplankton Data

The phytoplankton community includes a diverse array of microorganisms, which can move by sinking, floating, or swimming, but mostly passively drifting with sea currents [24]. According to several studies carried out in the Mediterranean Sea phytoplankton species have been divided into 2 main fractions based on size [52, 69]. The first fraction (picophytoplankton) includes phytoplankton populations less than 3 μm in size. This fraction consists of two phytoplankton domains: the picoprokaryotes domain represented by Synechococcus, Prochlorococcus HL (high light-adapted) and Prochlorococcus LL (low light-adapted), and the picoeukaryotes domain consisting mainly of Pelagophytes, Prymnesiophytes, and green algae [34, 52, 69, 86, 87]. The second fraction (nano- and micro-phytoplankton) includes phytoplankton populations larger than 3 μm. Picophyplankton accounts for approximately 80% (±10%) of the total chlorophyll in the Mediterranean Sea [69]. Nano- and micro-phytoplankton represent on average 20% of total chlorophyll, are uniformly distributed along the water column and are scarcely present in the Deep Chlorophyll Maximum (DCM) [34, 69].
The spatial segregation of different phytoplankton groups is mainly related to the physical and biological processes that command the competition and coexistence among these groups. For example, some phytoplankton populations move along the water column in response to seasonal changes in environmental variables, according to their ecological adaptation skills. In general, the

light intensity reduction as a function of depth is usually contrasted with an increasing nutrient concentration. The gradient of the limiting resources (light intensity and nutrient concentration) together with other environmental parameters and the specific group adaptability, are the main drivers that determine the composition of the phytoplankton population along the water column. Based on this, the 3D advection-diffusion-reaction model simulates the phytoplankton growth using the Michaelis-Menten formulas [37, 60] and considering the most limiting factor between light intensity and phosphate concentration [5, 34, 88]. In particular, the Michaelis-Menten formulas include the half-saturation constants for light intensity and phosphate concentration, K_{I_i} and K_{R_i}, which help define the specific biological response of each group to environmental variables. The half-saturation constants depend on the metabolism of the specific phytoplankton group considered. In particular, phytoplankton groups with higher values of K_{Ii} and K_{Ri} are less adapted to light and nutrients, respect to those with lower K_{I_i} and K_{R_i}.

In this work, the validation of model is performed by comparing the theoretical results with the experimental data on the total *chl-a* concentration, collected during the MedSudMed-08 oceanographic survey. Initially, the spatio-temporal distribution of phytoplankton abundances is reproduced by the 3D model. Afterwards, the theoretical phytoplankton abundances are converted into *chl-a* and *Dvchl-a* concentrations using the conversion coefficients obtained in previous works. Specifically, we exploit the *(Dv)chl-a* cellular content curves of picoeukaryotes and Prochlorococcus (HL and LL) [5, 34], which are obtained by high-performance liquid chromatography (HPLC) analysis on seawater samples collected between Cape Passero and Malta [52, 69]. The mean vertical profiles of *chl-a* per picoeukaryote cell and of *Dvchl-a* per Prochlorococcus cell were obtained by Brunet et al. [52]. Considering that Synechococcus have never been estimated in the Mediterranean Sea and assuming the oligotrophic conditions, the *chl-a* cellular content of Synechococcus is set to 1.18 fg *chl-a*·cell^{-1} in accordance with the value measured in the English Channel oligotrophic waters [68]. Finally, the contribution to the chlorophyll concentration due to the presence of nano- and micro-phytoplankton (> 3μm) is estimated in the whole domain by using the interpolation methods described in sections *The 3-D advection-diffusion-reaction model* and *Simulation setup*.

As a result of all these assumptions, the spatio-temporal behaviour of the total *chl-a* and *Dvchl-a* concentration is investigated in the Gulf of Sirte from 1 January 2007 to 31 December 2008.

Simulation setup

In this work, we simulated the three-dimensional distribution of the total chlorophyll concentration by using the advection-diffusion-reaction model, and compared these theoretical results with the experimental data collected in the Gulf of Sirte during July 2008. In order to simulate the total chlorophyll concentration, as a first step we set the spatial distribution of some environmental variables (concentration of phosphate, velocity field of marine currents and concentration of total chlorophyll associated with the nano-and micro-phytoplankton) using the experimental data collected in the Gulf of Sirte during the MedSudMed-08 oceanographic survey. In particular, the phosphate concentrations experimentally acquired in the eleven hydrological stations (empty squares in Figure S1) were initially linearly interpolated to fill the gaps and to obtain the vertical profile of this environmental variable at each sampling point. Next, the phosphate concentrations in the eleven hydrological stations and the two horizontal components of the velocity field acquired at the forty-two hydrological stations (red circles in Figure S1) were interpolated by kriging to generate forty regularly-spaced data grids, one for each of forty depth levels. Similarly, the horizontal distribution of the total *chl-a* concentration associated with the nano-and micro-phytoplankton, was reproduced by calculating the 20% of the fluorescence data acquired in each hydrological station, and interpolating the results obtained for the whole domain. Regarding the distribution along the water column, the total *chl-a* concentration was considered to be uniformly distributed vertically [5, 34]. The spatial distributions of interpolated variables by kriging methods were also used to fix the initial conditions for the advection-diffusion-reaction model.

Regarding the simulation setup, it is worth remembering that in this work the dynamics of incident light intensity (I_{in}) was also investigated. In particular, the temporal behaviour of the incident light intensity at the water surface was estimated using remote sensing data acquired in the barycentre of the Gulf of Sirte (see the NASA web site http://eosweb.larc.nasa.gov/sse/RETScreen/), and adopting the methods used in previous works [5, 6, 34].

As a second step, we set the values of the environmental and biological parameters in such a way as to guarantee the stability and convergence conditions for the numerical method used. The numerical values assigned to the biological and environmental parameters are shown in Table S1.

The horizontal and vertical turbulent diffusivities were fixed on the basis of the environmental conditions observed in the Gulf of Sirte, and in accordance with the theoretical findings obtained in previous works [34, 53, 62, 63]. In particular, vertical turbulent diffusivity (D_z) has been calibrated based on previous field observations, which indicate weakly mixed water column conditions within the Gulf of Sirte throughout the year [34, 53]. Furthermore, the vertical turbulent diffusivity was set to better reproduce the depth, width and magnitude of chlorophyll peaks in all hydrological stations. The vertical diffusivity showed a good agreement with the previously reported values in the weakly mixed waters condition [62]. The horizontal turbulent diffusivity was considered isotropic in the horizontal water plane (D_x=D_y), and fixed according to the values obtained by Massel [63] for large gulfs.

The biological parameters were set to typical values of the four phytoplankton populations investigated, in accordance with previous theoretical and experimental results [52, 57, 58, 69, 75, 76, 77]. The maximum specific growth rates (r_i) were set on the basis of the experimental results reported in previous works [57, 77], while the specific loss rates (m_i) were calculated on the basis of experimental data given in Refs. [56, 58, 77, 89]. The sinking velocities (v_i) and the nutrient recycling coefficients (ε_i) were fixed in agreement with the theoretical results obtained by other authors [54, 88]. In particular, the magnitudes of sinking velocities of the four picophytoplankton populations were set to the values obtained by Raven [57], while nutrient recycling coefficients are calculated by using the assimilation efficiencies previously estimated by Thingstad and Sakshaugh [89]. The nutrient contents of picophytoplankton groups ($1/Y_i$) were set to the same values as in a previous work [34]. Here, the nutrient contents for Synechococcus and picoeukaryotes were estimated using experimental results obtained by other authors [75, 76], while the nutrient content for the Prochlorococcus (both ecotypes) was set up to respect the ratios of the average concentrations of the picophytoplankton groups observed experimentally near the Gulf of Sirte [34, 52, 69].

The half-saturation constants (K_{I_i} and K_{R_i}) were set to the same values over the whole 3D domain. Specifically, the values of K_{I_i} and K_{R_i} were chosen within ranges reported in literature [34, 76, 77], performing a fine tuning to get the best agreement between the picophytoplankton abundances obtained from the model and those experimentally measured in the Strait of Sicily by other authors [52, 69].

Finally, the *chl-a*-normalized average absorption coefficients of phytoplankton populations (a_i) and the background turbidity (a_{bg}) were set at the same values of previous works [5, 34]. Overall, the average absorption coefficients used for phytoplankton populations were in agreement with the absorption coefficients measured by Brunet et al. [86] in the coastal areas around the Strait of Sicily.

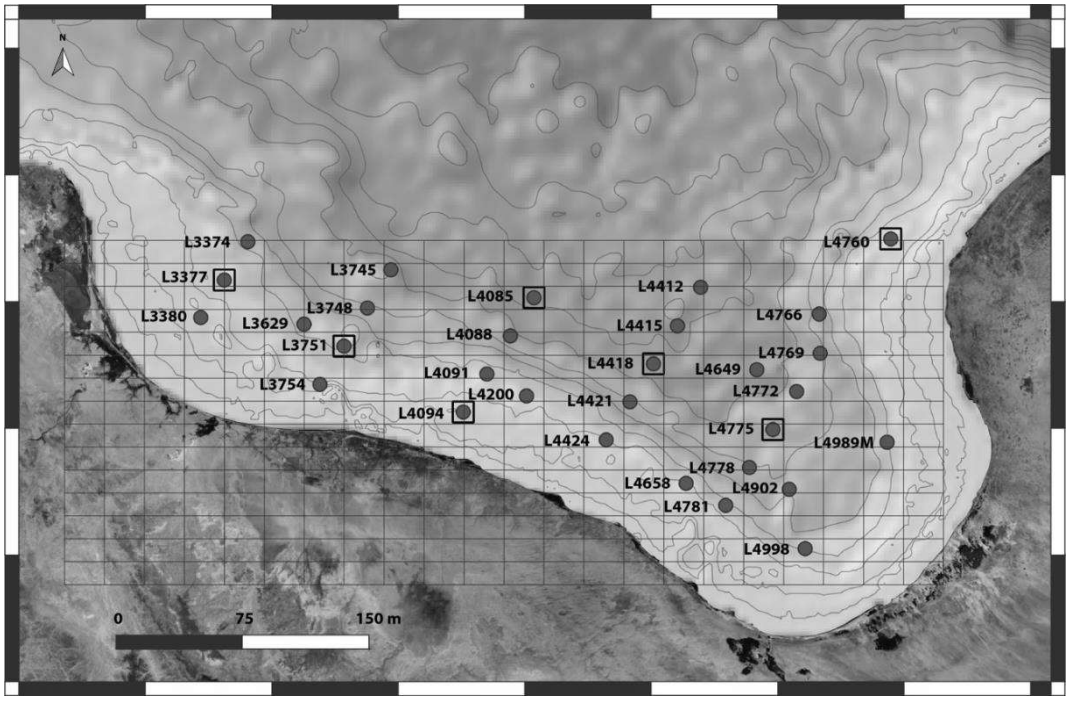

Fig. S1.

Geographic location of the model grid on the horizontal plane (16x23 cells) in the Gulf of Sirte. The grid also shows the location of the CTD stations (red circles) and the nutrients stations (empty squares). The bathymetric underlay and bathymetric contours (General Bathymetric Chart of the Oceans (GEBCO) web portal).

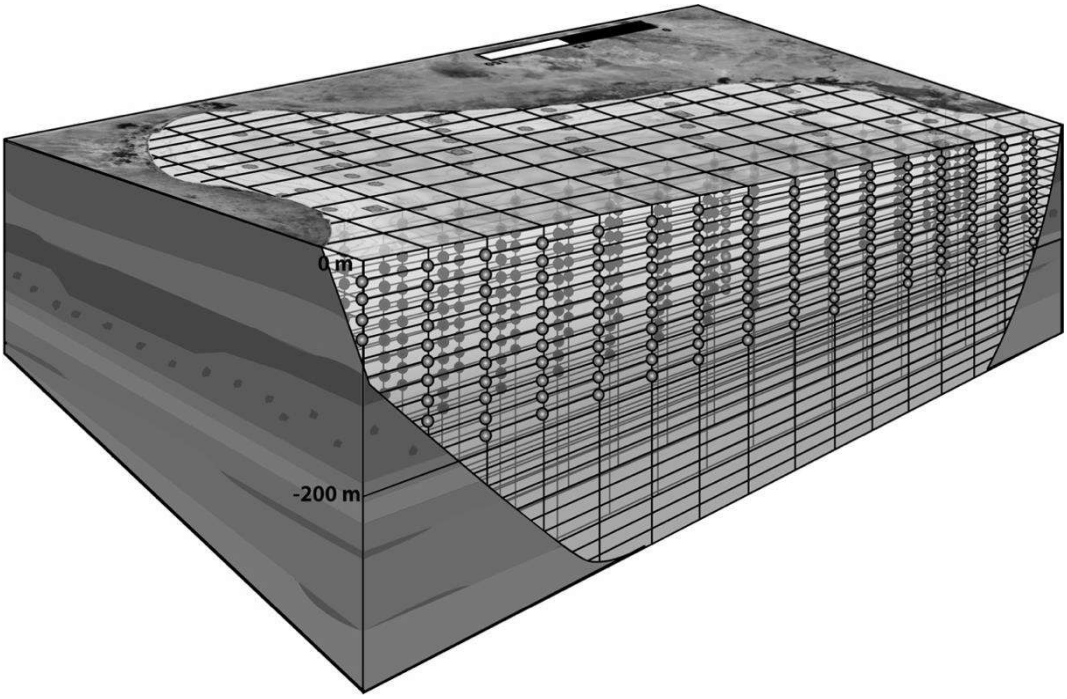

Fig. S2.

The 3D representation. The 3D representation shows the model grid and the position of simulated data points and in-situ observed CTD and nutrients stations points.

Symbol	Interpretation	Units	Value
a_{bg}	Background turbidity	m^{-1}	0.060
a_1	Average absorption coefficient of Synechococcus	$m^2 \cdot mg \cdot chl\text{-}a^{-1}$	0.025
a_2	Average absorption coefficient of Prochlorococcus HL	$m^2 \cdot mg \cdot chl\text{-}a^{-1}$	0.016
a_3	Average absorption coefficient of picoeukaryotes	$m^2 \cdot mg \cdot chl\text{-}a^{-1}$	0.012
a_4	Average absorption coefficient of Prochlorococcus LL	$m^2 \cdot mg \cdot chl\text{-}a^{-1}$	0.027
a_5	Average absorption coefficient of phytoplankton > 3µm	$m^2 \cdot mg \cdot chl\text{-}a^{-1}$	0.020
r_1	Maximum specific growth rate of Synechococcus	h^{-1}	0.058
r_2	Maximum specific growth rate of Prochlorococcus HL	h^{-1}	0.088
r_3	Maximum specific growth rate of picoeukaryotes	h^{-1}	0.096
r_4	Maximum specific growth rate of Prochlorococcus LL	h^{-1}	0.031
K_{I_1}	Half-saturation constant of light-limited growth of Synechococcus	$\mu molphotons \cdot m^{-2} \cdot s^{-1}$	130
K_{I_2}	Half-saturation constant of light-limited growth of Prochlorococcus HL	$\mu molphotons \cdot m^{-2} \cdot s^{-1}$	64.5
K_{I_3}	Half-saturation constant of light-limited growth of picoeukaryotes	$\mu molphotons \cdot m^{-2} \cdot s^{-1}$	36.5
K_{I_4}	Half-saturation constant of light-limited growth of Prochlorococcus LL	$\mu molphotons \cdot m^{-2} \cdot s^{-1}$	0.8
K_{R_1}	Half-saturation constant of nutrient-limited growth of Synechococcus	$mmol\ phosphorus \cdot m^{-3}$	0.03
K_{R_2}	Half-saturation constant of nutrient-limited growth of Prochlorococcus HL	$mmol\ phosphorus \cdot m^{-3}$	0.09
K_{R_3}	Half-saturation constant of nutrient-limited growth of picoeukaryotes	$mmol\ phosphorus \cdot m^{-3}$	0.13
K_{R_4}	Half-saturation constant of nutrient-limited growth of Prochlorococcus LL	$mmol\ phosphorus \cdot m^{-3}$	0.15
m_1	Specific loss rate of Synechococcus	h^{-1}	0.014
$m_2=m_4$	Specific loss rate of Prochlorococcus	h^{-1}	0.011
m_3	Specific loss rate of picoeukaryotes	h^{-1}	0.010
$1/Y_1$	Nutrient content of Synechococcus	$mmol\ phosphorus \cdot cell^{-1}$	$2.0 \cdot 10^{-12}$
$1/Y_2=1/Y_4$	Nutrient content of Prochlorococcus	$mmol\ phosphorus \cdot cell^{-1}$	$4.0 \cdot 10^{-13}$
$1/Y_3$	Nutrient content of picoeukaryotes	$mmol\ phosphorus \cdot cell^{-1}$	$2.0 \cdot 10^{-12}$
c_1	Chl-a cellular content of Synechococcus	$fg.chl\text{-}a \cdot cell^{-1}$	1.18
$c_2=c_4$	Dvchl-a cellular content of Prochlorococcus	$fg.Dvchl\text{-}a \cdot cell^{-1}$	0.25 - 2.20
c_3	Chl-a cellular content of picoeukaryotes	$fg.chl\text{-}a \cdot cell^{-1}$	10.0 - 660.0
ε_1	Nutrient recycling coefficient of Synechococcus	dimensionless	0.51
$\varepsilon_2=\varepsilon_4$	Nutrient recycling coefficient of Prochlorococcus	dimensionless	0.52
ε_3	Nutrient recycling coefficient of picoeukaryotes	dimensionless	0.52
v_1	Magnitude of sinking velocity of Synechococcus	$m \cdot h^{-1}$	0.000088
$v_2=v_4$	Magnitude of sinking velocity of Prochlorococcus	$m \cdot h^{-1}$	0.000039
v_3	Magnitude of sinking velocity of picoeukaryotes	$m \cdot h^{-1}$	0.000098
v_x	Horizontal velocity along x-axis	$m \cdot h^{-1}$	0.00 – 1.47
v_y	Horizontal velocity along y-axis	$m \cdot h^{-1}$	0.00 – 1.12
v_z	Vertical component of velocity field	$m \cdot h^{-1}$	0.0
$D_x=D_y$	Horizontal turbulent diffusivity	$km^2 \cdot h^{-1}$	36.0
D_z	Vertical turbulent diffusivity	$m^2 \cdot h^{-1}$	1.2
I_{in}	Incident light intensity at the surface water	$\mu molphotons \cdot m^{-2} \cdot s^{-1}$	518.3 - 1713.7
R_{in}	Nutrient concentration at the domain boundaries	$mmol\ phosphorus \cdot m^{-3}$	0.010 - 0.110
z_b	Depth of the water column	m	0 - 200

Table S1.

Parameters and variables used for the 3D model. The values of the environmental and biological parameters are those typical of four phytoplankton populations that coexist in the in the Gulf of Sirte.

Credit Author Statement: RF, SG, SA, SM, AB, SZ, GB conceived and designed the experiments; RF, SG, SA, AB, GB, SZ, GG, IF performed the experiments; HA, SA, DV, GD developed the numerical models; HA, SA, GD, GB analysed the data and interpreted results; HA, SA, GD wrote the paper; HA, SA, GD, GB, DV, AB, BS, SM substantively revised the manuscript.